Research article

JGS
Journal of the Geological Society

https://doi.org/10.1144/jgs2022-133 | Vol. 180 | 2023 | jgs2022-133

Mid-Ordovician stratigraphy and volcanism in the Hølonda area, Scandinavian Caledonides: complex tectonomagmatic development following arc–continent collision near the Laurentian margin of Iapetus

Tor Grenne[1]*, Deta Gasser[1,2], Reidulv Bøe[1], Fernando Corfu[3], Øyvind Skår[1] and Trond Slagstad[1]

[1] Geological Survey of Norway, PO Box, 6315 Torgarden, 7491 Trondheim, Norway
[2] Department of Environmental Sciences, Western Norway University of Applied Sciences, Røyrgata 6, 6856 Sogndal, Norway
[3] Department of Geosciences and CEED, University of Oslo, PO Box 1047, Blindern, 0316 Oslo, Norway
DG, 0000-0001-7300-8984; RB, 0000-0002-9486-3530; FC, 0000-0002-9370-4239; ØS, 0000-0001-9174-490X; TS, 0000-0002-8059-2426
* Correspondence: tor.grenne@ngu.no

Abstract: The Hølonda area of the central Scandinavian Caledonides is a key for models of the Caledonian orogen owing to its Ordovician fauna of Laurentian affinity, now stranded on the Baltic side during opening of the North Atlantic. Here, we present a revised stratigraphic and tectonomagmatic model based on remapping, sedimentology, igneous geochemistry, Nd and Sr isotopes and geochronology. The Hølonda Group (*c.* 470–461 Ma) reflects a transition from subaerial and shallow-marine deposition on a continental shelf to deeper-water sedimentation along a subsiding slope. Adakitic and mid-ocean ridge basalt type magmatism at *c.* 468 Ma was succeeded by benmoreitic–rhyolitic, shoshonitic, calc-alkaline and ultra-alkaline volcanism at *c.* 467–465 Ma. The complex magmatism followed arc–continent collision along a microcontinent outboard of Laurentia, associated with subduction polarity flip and slab rollback. This led to rifting and opening of a wide basin and its adjoining shelf on thickened orogenic lithosphere. Associated mantle upwelling and partial melting of depleted and variably metasomatized mantle occurred in a tectonomagmatic setting comparable with that of the central Mediterranean. The Hølonda–Ilfjellet setting is unique along the Caledonian–Appalachian orogen, possibly reflecting interaction with Laurentia-derived continental terranes at the northeastern end of the Taconian–Grampian orogenic tract.

Supplementary material: Analytical data and supplementary figures are available at https://doi.org/10.6084/m9.figshare.c.6368922

Thematic collection: This article is part of the Caledonian Wilson cycle collection available at: https://www.lyellcollection.org/topic/collections/the-caledonian-wilson-cycle

Received 21 September 2022; **revised** 22 December 2022; **accepted** 3 January 2023

The Iapetus Ocean, which existed between the continents Laurentia, Baltica and Amazonia in the late Neoproterozoic to early Paleozoic, was one of the major oceanic basins of the Phanerozoic (Wilson 1966; Harland and Gayer 1972; Domeier 2016; Robert *et al.* 2021). Its existence was originally proposed based on the presence of widely different faunal realms within the Scandinavian Caledonides, with the Hølonda area in the central Scandinavian Caledonides playing a key role (Fig. 1; Wilson 1966; Gee 1975; Bruton and Bockelie 1982; Pedersen *et al.* 1992; Harper *et al.* 1996, 2009). Here, a rich and well-preserved Ordovician fossil fauna was discovered by Brøgger (1875) and Kjerulf (1981), and further studied by Kjær (1932) and Strand (1949). Subsequent studies of graptolites, brachiopods, trilobites and conodonts from limestones and shales demonstrated an unequivocal Laurentian affinity for these fossils (Blake 1962; Neuman and Bruton 1974, 1989; Bergström 1979; Bruton and Bockelie 1980; Schmidt 1984); the additional presence of brachiopods that were not known from Laurentia indicated that the Hølonda rocks formed offshore of the main Laurentian continent in an oceanic setting (Neuman and Bruton 1989). Comparable Laurentian fossil faunas are also known from the island of Smøla, *c.* 90 km west of Hølonda, and in the Snåsa area, *c.* 170 km NE of Hølonda (Fig. 1a; Roberts 1980, 1982*a*, *b*, 1998).

Vogt (1945) established a stratigraphic scheme for the Hølonda region, dividing the area into two main units, the Støren and the overlying Lower Hovin Series, which were later generally referred to as groups (e.g. Bruton and Bockelie 1980). Chaloupsky (1970) proposed a new stratigraphic terminology for the area, with the Krokstad Group replacing the Lower Hovin Group; however, the stratigraphic terminology of Vogt (1945) was mainly retained in subsequent studies, which dealt with either the classification of fossils (Neuman and Bruton 1974, 1989; Bergström 1979; Bruton and Bockelie 1980) or the igneous geochemistry of porphyrites (Grenne and Roberts 1998).

Despite the importance of the Hølonda fossil fauna for palaeogeographical and palaeotectonic reconstructions, a modern evaluation of their stratigraphic framework and volcanic evolution has been lacking. Recently, Gasser *et al.* (2021) defined the stratigraphy and volcanic history of the adjacent Ilfjellet Group (*c.* 474–463 Ma; Fig. 1b), pointing at a palaeogeographical link between the Ilfjellet and Hølonda successions. Building on that study, we present a detailed remapping of the Hølonda area combined with geochemical, isotopic and geochronological data from newly discovered volcanic units, detrital zircon data from the metasedimentary succession and a reassessment of the well-known

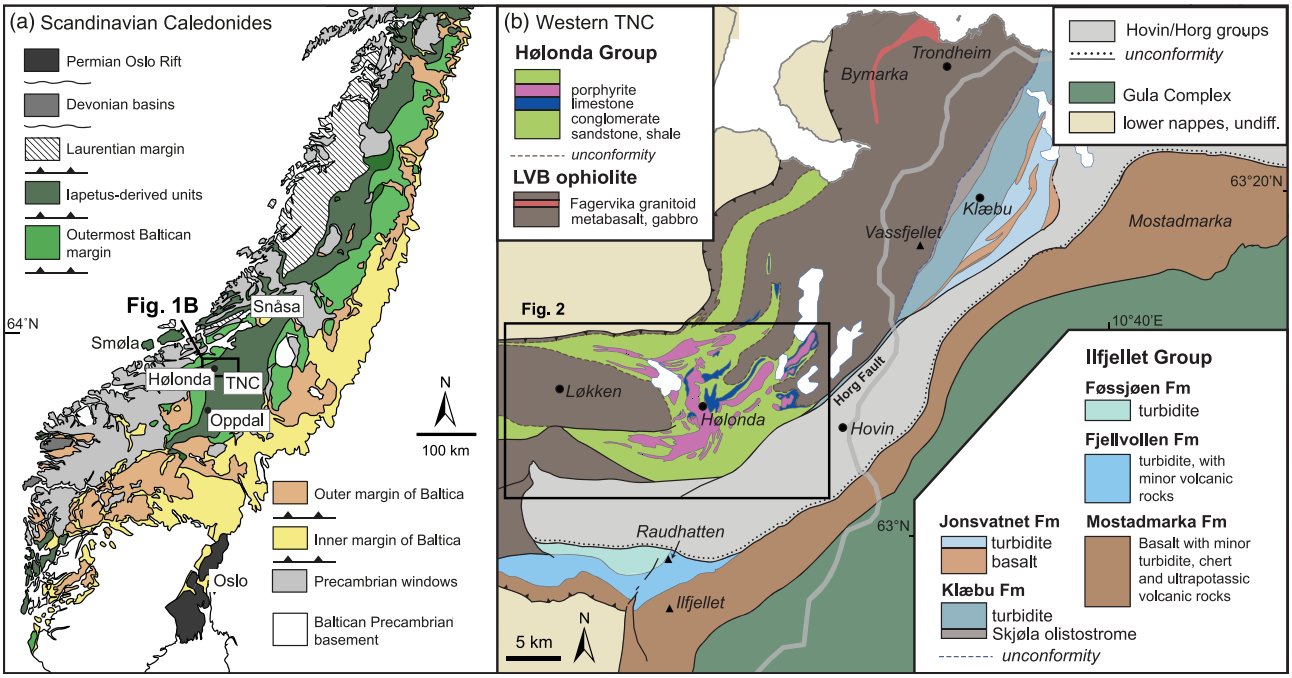

Fig. 1. (**a**) Overview map of the Scandinavian Caledonides. TNC, Trondheim Nappe Complex. (**b**) Geological map of the western TNC, modified from Gasser *et al.* (2021).

porphyrites. Based on these data, we propose a revised stratigraphic framework and a new interpretation of the depositional and palaeotectonic evolution of the Hølonda area, taking into account correlative successions of the adjacent Ilfjellet Group (Gasser *et al.* 2021), and the Trollhøtta and Skarvatnet units (*c.* 474–470 Ma) in the Oppdal area farther south (Fig. 1a; Dalslåen *et al.* 2020, 2021*b*).

Regional setting

The Hølonda area is situated in the western parts of the Trondheim Nappe Complex, which is preserved within a large-scale NNE–SSW-trending synform (Fig. 1a; Roberts and Wolff 1981; Gee *et al.* 1985). Here, Ordovician sedimentary and volcanic rocks that are assigned in the present paper to the newly defined Hølonda Group rest unconformably on a basement of ophiolite fragments referred to as the Løkken–Vassfjellet–Bymarka (LVB) ophiolite (Fig. 1b; Furnes *et al.* 1980; Grenne 1980, 1989; Heim *et al.* 1987). Geochemically, the ophiolite shows suprasubduction-zone signatures characteristic of oceanic-arc-related marginal basins (Slagstad 2003; Slagstad *et al.* 2014). U–Pb zircon dating of comagmatic plagiogranites constrains the formation age of the ophiolite to *c.* 487–480 Ma (Roberts and Tucker 1998; Roberts *et al.* 2002; Gromet and Roberts 2010, 2016; Slagstad *et al.* 2014). Its lowest preserved parts comprise sporadic ultramafic cumulates; basal parts are not preserved owing to later (Scandian) folding and thrusting and younger faulting (Fig. 1b).

The LVB ophiolite is generally interpreted to have been obducted onto an unknown continental basement near the Laurentian margin of Iapetus during arc–continent collision shortly after its formation in late Cambrian to early Ordovician times (e.g. Slagstad *et al.* 2014; Gasser *et al.* 2021). Prior to deposition of the Hølonda Group, the LVB ophiolite was subject to subaerial oxidative weathering, as reflected by variably penetrative, hematitic alteration. At Løkken, the ophiolite was cut by thin felsic dykes characterized by small phenocrysts of plagioclase and sporadic hornblende and partially resorbed quartz, dated at 468.2 ± 0.7 Ma, similar to intrusive rocks near Trondheim dated at 467.4 ± 4.9 Ma (Slagstad *et al.* 2014). A swarm of SSW–NNE-trending, steeply WNW-dipping, porphyrite dykes with individual thickness up to at least 40 m also cuts the ophiolite at Løkken (Grenne 1989).

At Vassfjellet (Fig. 1b), the LVB ophiolite is unconformably overlain by turbidites and volcanic rocks of the Ilfjellet Group, which represents the development of a major rift basin from *c.* 474 Ma onwards (Gasser *et al.* 2021; Smelror *et al.* 2022). The upper part of this succession (the Raudhatten unit of the Fjellvollen Formation) contains highly distinctive conglomerates and breccias with abundant debris of porphyrite, providing a palaeogeographical link between the Ilfjellet and the Hølonda successions (Gasser *et al.* 2021). The Ilfjellet Group contains a peculiar association of depleted to enriched mid-ocean ridge basalts (D- to E-MORB) and extremely Th-rich, ultrapotassic volcanic rocks. Farther south, near Oppdal (Fig. 1a), the Trollhøtta and Skarvatnet units comprise a similar turbidite succession intercalated with MORB and shoshonitic to ultrapotassic volcanic rocks (Dalslåen *et al.* 2020, 2021*a*).

The Hølonda area is tectonically separated from the younger (*c.* 460–420 Ma) Hovin and Horg groups by the Horg Fault (Fig. 1b), whereas the Ilfjellet Group is in tectonic contact with the Gula Complex in the east and unconformably overlain by the Hovin and Horg groups in the west (Fig. 1b).

Field relationships of the Hølonda Group

We investigated the mid-Ordovician, lower greenschist-facies, sedimentary and volcanic succession of the Hølonda area from Storås in the west to Grøtvatnet in the east, concentrating on well-preserved strata south and east of Svorksjøen (Fig. 2). It should be noted that the place name Hølonda has earlier been used to designate limestones, porphyrites and shales in the area (e.g. Vogt 1945). Following recommendations for stratigraphic terminology (Nystuen 1989), we restrict the use of the Hølonda name for the entire group as described in this contribution.

Structural relationships

The Hølonda Group occurs in two tectonic units, separated by the generally SW–NE-trending and NW-dipping Frillsjøen–Grøtvåttån fault (Fig. 2). To the NW, in the central Hølonda area, it comprises

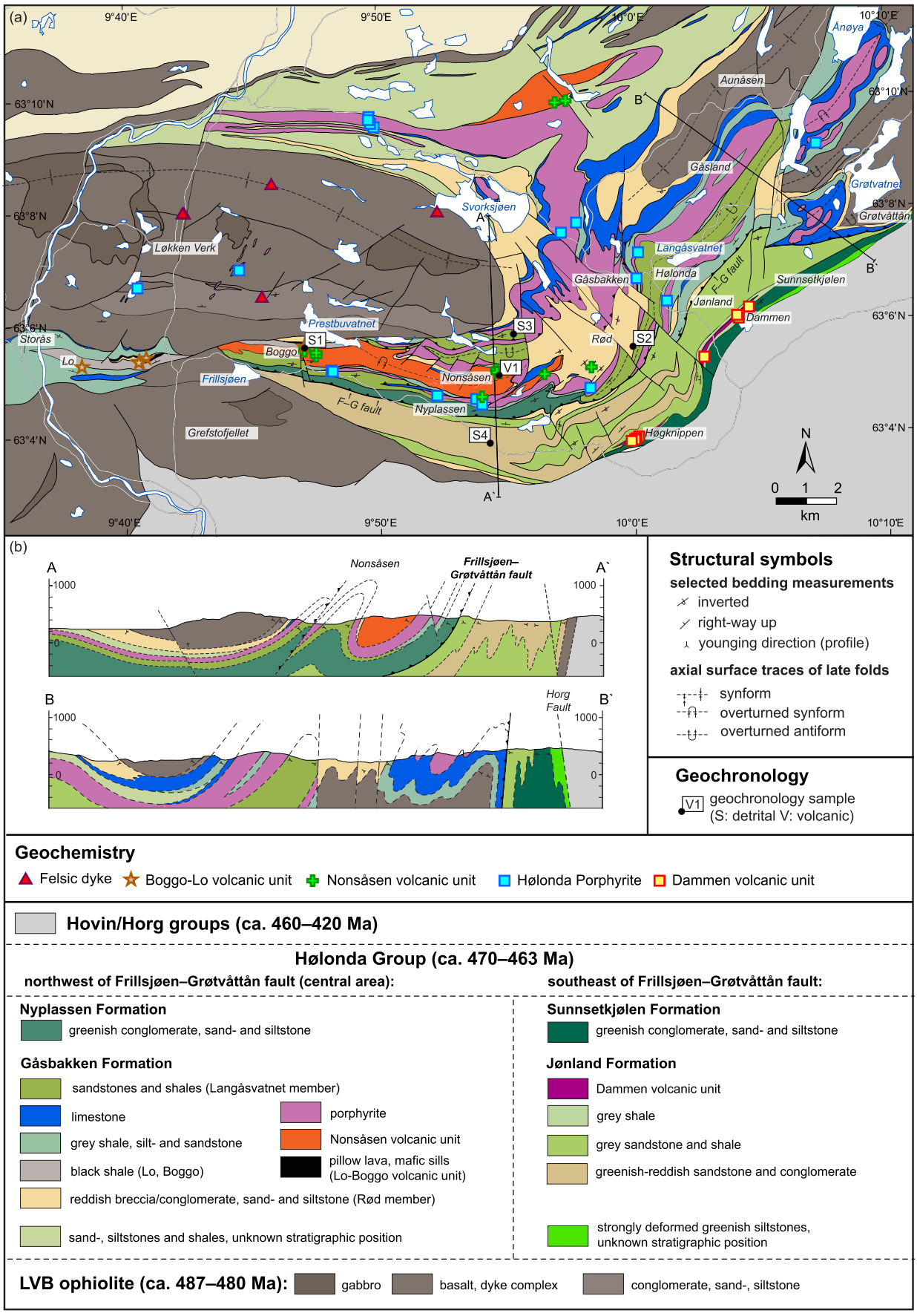

Fig. 2. (**a**) Detailed geological map of the Hølonda area, following the new stratigraphic terminology of the present study. Sample localities for geochronology and geochemistry are indicated. F, Frillsjøen; G, Grøtvåttån. (**b**) Simplified geological profiles through the western and eastern parts of the study area.

the Gåsbakken and Nyplassen formations. Here, the overall structure is controlled by a large-scale recumbent fold nappe. The inverted limb is preserved in northwestern parts, where volcanic (pillow lava) and sedimentary (graded bedding, channelling, etc.) way-up indicators demonstrate that the ophiolite fragments at Løkken and Aunåsen as well as the younger Hølonda Group rocks are consistently inverted (Fig. 2a and b). The normal limb is present in the eastern parts, around Grøtvatnet–Ånøya, where the Hølonda Group overlies the ophiolite in an upright position (Fig. 2b).

To the SE of the Frillsjøen–Grøtvåttån fault, in the southeastern Hølonda area, the Hølonda Group comprises the Jønland and Sunnsetkjølen formations (Fig. 2), which are interpreted as stratigraphic equivalents of the Gåsbakken and Nyplassen formations (Fig. 3). Bedding in this tectonic unit dips moderately to steeply to the NW. Tight to isoclinal mesoscale folds are common (Fig. 2b), but way-up indicators and stratigraphic correlations generally indicate younging towards the south and SE. The unit is bordered to the SE by the Horg and related younger faults (Fig. 2).

Gåsbakken Formation

The Gåsbakken Formation, comprising the stratigraphically lower part of the Hølonda Group, is characterized by redbeds, grey shale and sandstone, limestone and a variety of volcanic units, including the previously studied porphyrites (Grenne and Roberts 1998). Large facies variations are observed along-strike and many of the individual members are found only in parts of the area (Fig. 3).

Rød redbeds

Redbed type breccias, conglomerates and finer-grained sedimentary rocks, lithologies previously termed Gaustadbakk breccia and Almås mudstone, respectively (Vogt 1945), are common in lower parts of the Gåsbakken Formation, locally overlying purplish pillow lavas of the ophiolite's palaeo-weathering surface (e.g. near Gåsland; Figs 2 and 3). Including lithologically similar but greyish varieties, the redbed succession is informally referred to as the Rød member based on its greatest extent of excellent exposure in the Rød area (Fig. 2). Here it is up to *c.* 1 km thick, whereas it is missing in other places (Fig. 3).

The Rød breccias and conglomerates are characterized by clasts of volcanic rocks variably affected by oxidative weathering, along with varying proportions of jasper, limestone and quartzite, commonly in a purplish mudstone matrix (Fig. 4a–c). Abundant felsic clasts are generally plagioclase-phyric and moderately amygdaloidal.

Sedimentary facies characteristics include trough cross-bedding and planar lamination in gravel–pebble (clasts <2 cm) conglomerates/breccias up to 1 m thick. Coarse beds are commonly normally graded, with erosive lower boundaries (shallow channels) and many rip-up clasts of siltstone; clast imbrication is observed in places (Fig. 4d). Sandy and silty interbeds up to 0.7 m thick show planar lamination and ripples and pass upwards into finer-grained sediments with centimetre-thick mudstone layers and lenticular bedding (Fig. 4e). Some thin-bedded, normally graded fine sandstone–shale units show laterally extensive, regular beds (Fig. 4f) with erosive bases and parallel-laminated tops.

Lo–Boggo volcanic unit and associated sedimentary succession

In places, the redbed deposits pass into and are interbedded with grey sandstone and gravel conglomerate and grey to black shale. In the western part of the study area, near Boggo (Figs 2 and 3), a succession of quartz-rich sandstone and conglomerate includes abundant black shale and associated thin beds of gritty limestone intercalated with mafic volcanic rocks. Grading and channelling are common in sandy and conglomeratic beds. According to Blake (1962) and Schmidt (1987), the total shale thickness at Boggo amounts to 40–60 m. Farther west, equivalent black shales at Lo (Fig. 2) are associated with local pillow lava and mafic sills. The black shales at Boggo and Lo are known for their profuse graptolite fauna of mid-Ordovician, mostly early Darriwilian age (Ryan *et al.* 1980; Schmidt-Gündel 1994), the oldest Lo graptolites possibly dating back to Castlemainian 1 (Schmidt-Gündel 1994) at *c.* 470 Ma (Cohen *et al.* 2013). In the following, we refer to the mafic volcanic rocks at Lo and Boggo as the Lo–Boggo volcanic unit.

Nonsåsen volcanic unit

At Boggo, the above-described succession is overlain by previously unrecognized volcanic rocks, here referred to as the Nonsåsen volcanic unit (Fig. 2). Mapped as 'greenstone conglomerate' by Chaloupsky (1977), this unit has a lateral extent of at least 10 km and a maximum thickness of several hundred metres. It occurs in the core of a major anticlinal synform from Prestbuvatnet to Nonsåsen and is intercalated with a predominantly up-towards-south

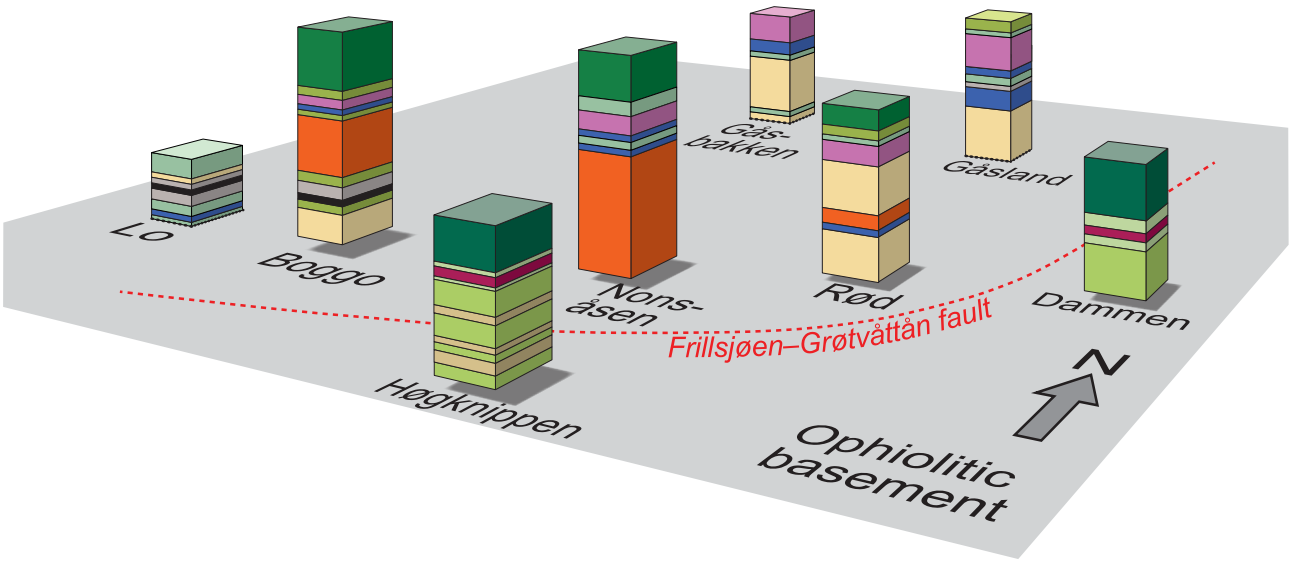

Fig. 3. Stratigraphic columns highlighting lateral facies and thickness variations across the study area. For colour legend, see Fig. 2.

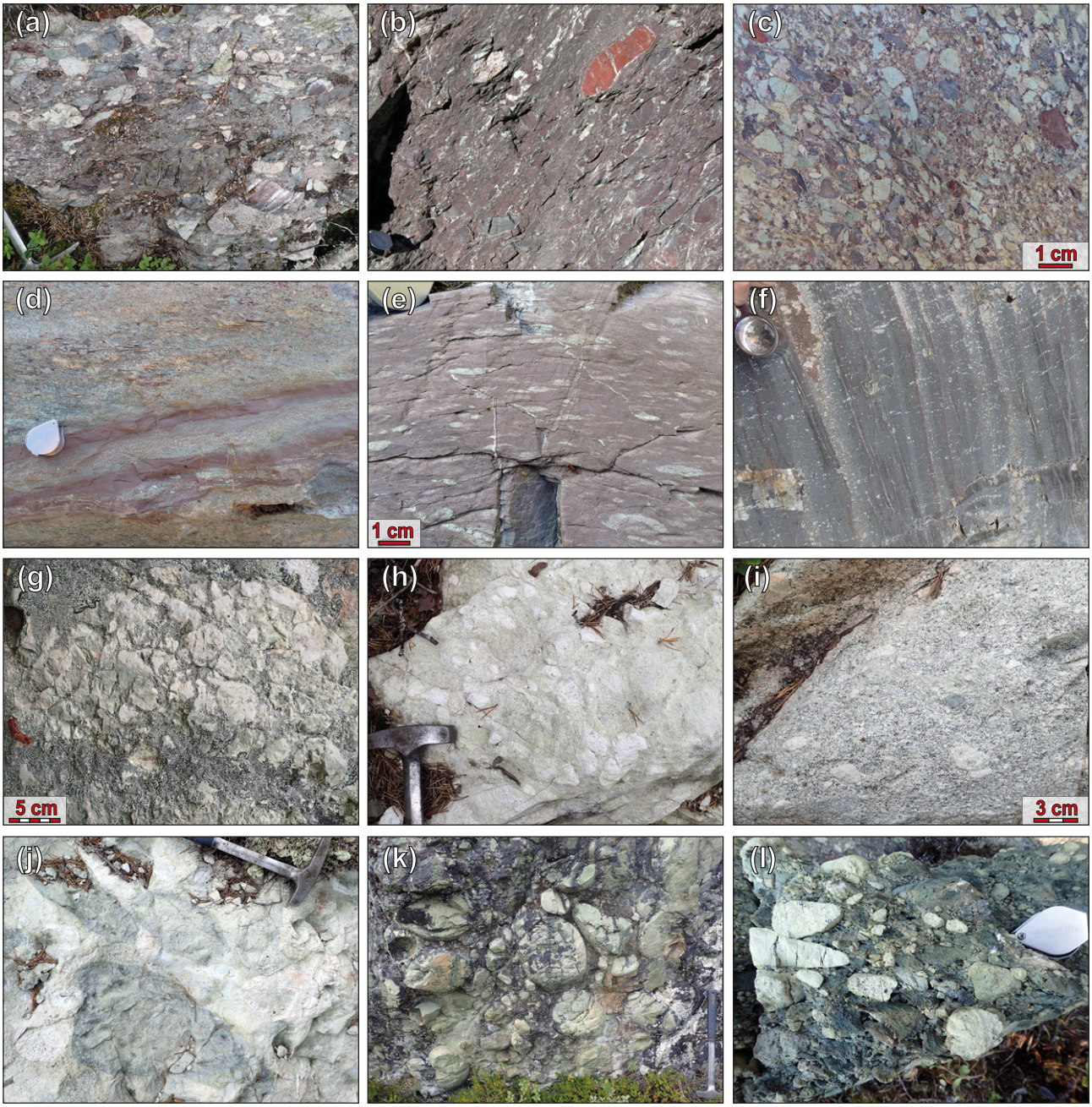

Fig. 4. Field photographs, lower parts of the Gåsbakken Formation. Locations are given in UTM coordinate system WGS84, zone 32. (**a**) Redbed (Rød member) breccia (E549368/N6995321). (**b**) Redbed breccia with red and green clasts of basalt, and a jasper clast, in red mudstone matrix (E551193/N6996349). (**c**) Redbed pebble/granule breccia (E550454/N6996345). (**d**) Redbed pebble–granule breccia alternating with sandstone and red silt–mudstone. Note normal grading in sandstones and sharp, erosive boundaries between mudstones and overlying coarser sediments (E550454/N 6996345). (**e**) Redbed siltstone–mudstone with sand lenses (lenticular bedding) (E549108/N6995719). (**f**) Normally graded beds of redbed siltstone–shale (E554955/N7000847). (**g**) Nonsåsen, autobrecciated andesitic lava (E545539/N6994745). (**h**) Nonsåsen, autobrecciated andesitic lava (E545977/N6995187). (**i**) Nonsåsen, andesitic tuff with irregular and subangular volcanic and sporadic lithic clasts (E545855/N6995272). (**j**) Nonsåsen, volcanic bombs (E546430/N6994800). (**k**) Nonsåsen, conglomerate with rounded cobbles and boulders between lava flows (E546169/N6994822). (**l**) Conglomerate on top of the Nonsåsen volcanic unit (E543866/N6994891).

succession of Rød redbeds and limestones east of a major fault in the Rød area (Fig. 2). The unit tapers northeastwards and is absent at stratigraphically equivalent levels in the Gåsland and Grøtvatnet areas (Figs 2 and 3).

The Nonsåsen volcanic unit is dominated by light grey, flinty, fine-grained intermediate to felsic rocks. Non- or moderately amygdaloidal types predominate, typically with abundant 1–2 mm phenocrysts of plagioclase and varying proportions of brown hornblende; augitic clinopyroxene is subordinate. Parts of the unit comprise alternating coherent and autobrecciated lava with angular fragments in a compositionally similar matrix (Fig. 4g and h). Other parts are dominated by lapilli tuff, comprising fine-grained volcanic material with irregular and subangular volcanic and sporadic lithic clasts (Fig. 4i) or, locally, bombs (Fig. 4j); subordinate crystal tuff displays a faint, metre-scale bedding. Internal beds of clast-supported conglomerate comprise large, rounded cobbles and boulders of Nonsåsen-like volcanic rocks in a felsic tuffaceous matrix (Fig. 4k); angular to subangular limestone clasts are abundant in places.

In places, the Nonsåsen volcanic unit is overlain by a poorly sorted conglomerate with sub-angular to sub-rounded Nonsåsen-type volcanic clasts and minor jasper and volcanic rocks (Fig. 4l).

This passes upwards into graded sandstones and granule conglomerates, in which the predominant detritus is quartz, feldspar and carbonate. At its eastern end, the volcanic unit is overlain by another 300–400 m of redbeds (Fig. 3).

Limestone and shale

South of Nonsåsen (Fig. 2), a thin limestone rests directly on the volcanic deposits or on volcanic-derived conglomerates. Palaeokarst (Fig. 5a) is observed locally. The limestone is overlain by grey shale and, in turn, thicker limestone. A similar sequence of two limestones separated by shale (partly black) is seen near Gåsland (Figs 2 and 3), where the Nonsåsen volcanic unit is missing and the lower limestone rests directly on Rød redbeds. The limestones are well- to indistinctly bedded (Fig. 5b), including both micritic and richly fossiliferous varieties (Fig. 5c). The shales typically have lenses and ripples of fine sand 0.5–2 cm thick, alternating with intervals of flaser bedding. Sandy beds <10 cm thick with planar lamination, cross-bedding and current ripples are subordinate (Fig. 5d).

Brachiopods, trilobites, molluscs and cystoids are abundant (Neuman and Bruton 1974, 1989). Bergström (1979) showed that conodonts in the limestones are similar to those of the Anomalorthis Zone of the Antelope Valley Limestone in Nevada and suggested that they were time equivalents of middle Kundan strata in the Baltic area, i.e. *c.* 466–465 Ma, according to modern chronostratigraphy (Cohen *et al.* 2013).

Porphyrites

Porphyrites occur through most of the study area (Figs 2 and 3), particularly between underlying limestone and overlying shale and sandstone. The porphyrite units vary in thickness from tens of metres to at least 700 m, in places being virtually uninterrupted over a thickness of at least 120 m. They comprise mafic to subordinate intermediate igneous rocks characterized by varying proportions of tabular plagioclase and clinopyroxene (augite) phenocrysts in a microcrystalline matrix (Fig. 5e and f); varieties dominated by clinopyroxene predominate in the SW. Phenocrysts are up to 1 cm in interior parts of the units but significantly smaller near the upper and lower contacts, where flow breccia-like structures also occur. Flow banding is commonly represented by subparallel aligned phenocrysts. Moderately amygdaloidal varieties (Fig. 5f) are particularly common at the top of porphyrite units. Pillows, hyaloclastites and other features typical of submarine flows are absent.

Contacts with stratigraphically underlying limestone commonly show breccia-like structures (Fig. 5g), where remains of limestone with irregular and highly embayed outlines are set in a coherent matrix of fine-grained porphyrite. By contrast, the stratigraphic upper surfaces of the porphyrites have sharp and regular contacts with overlying shale and sandstone, locally showing a slightly undulating surface with a thin (*c.* 1 cm) originally glassy margin (Fig. 5h).

Langåsvatnet sandstones and shales

The porphyrites are overlain by a few tens of metres of thin-bedded (up to 10 cm, but typically <5 cm) grey sandstone and shale (Fig. 5i). Beds can be traced for several metres, exhibiting planar lamination, cross-lamination, hummocky cross-bedding and, locally, disrupted bedding or soft sediment deformation, possibly in channels. Upwards, this interval passes into grey, fine- to medium-grained sandstones and shales with planar lamination, cross-bedding, ripples and ball-and-pillow structures. Informally referred to as the Langåsvatnet member, this succession reaches up to 300 m in thickness in the Næve and Langåsvatnet areas (Figs 2 and 3).

Nyplassen Formation

The Nyplassen beds were originally defined by Chadwick *et al.* (1963) to include the entire sedimentary succession between porphyrites, limestones and shales in the north and the Grefstofjellet ophiolite fragment in the southwestern part of the study area (Fig. 2). Here we define the Nyplassen Formation to include only the sedimentary succession between the Gåsbakken Formation in the north and the Frillsjøen–Grøtvåttån Fault in the south (Fig. 2). The Nyplassen Formation is composed primarily of greenish, bedded (typically 10–50 cm) sandstones, siltstones and granule conglomerates (Fig. 5j and k). As in the underlying Gåsbakken Formation, the sedimentary rocks are quartz-rich, but they are less calcareous and have significantly more of a mafic component (Fig. 5l). Sedimentary structures include normal grading, planar and cross-bedding in sandstones, and planar and cross-lamination in siltstones. Erosion surfaces and shallow channels are common. Volcanic or intrusive rocks have not been observed.

According to Ryan *et al.* (1980) the Nyplassen Formation has yielded graptolites of mid-Darriwilian age (Da2 and Da3); that is, within the range of *c.* 466–461 Ma. The fossil locality at Nyplassen (UTM32 E544245/N6994160, P. D. Ryan, pers. comm. 2022) is within the Nyplassen Formation as defined also in the present paper (Fig. 2).

Jønland Formation

We assign most of the sedimentary succession south and SE of the Frillsjøen–Grøtvåttån Fault to the Jønland Formation (Fig. 2), comprising predominantly thin-bedded (<5 cm) grey, quartz–feldspar-rich and variably calcareous, fine-grained sandstone and shale (Fig. 6a); thicker sandstone beds (up to 50 cm) are subordinate. Normal grading, planar and cross-lamination and hummocky cross-lamination are common. Beds of breccia with clasts of jasper, quartzite and felsic volcanic rocks like the Rød redbeds occur locally. Towards west–SW, this unit passes laterally into a compositionally similar succession with increasing abundance of coarser beds, including granule conglomerates and redbed breccia and conglomerate (Fig. 6b).

This succession is interpreted as a lateral equivalent of the lower part of the Gåsbakken Formation owing to the intercalation of redbed type deposits (Fig. 3). It is stratigraphically overlain towards the SE by grey shale with fine sandstone lenses and beds of sandstone <8 cm thick with normal grading, soft sediment deformation, planar and cross-lamination and hummocky cross-lamination, and further finely laminated shale and siltstone with centimetre-thick layers and lenses of fine sandstone. A thin but distinctive volcanic unit, here referred to as the Dammen volcanic unit, appears sporadically along-strike interbedded with the shales. It comprises mostly intermediate, moderately amygdaloidal lava (Fig. 6c); spherulitic and macro-perlitic structures are seen in places. At Dammen (Fig. 2), intermediate lava is stratigraphically overlain by amygdaloidal (up to *c.* 50%) pillow basalt (Fig. 6d), separated by *c.* 5 m of shale.

Sunnsetkjølen Formation

The shales and local volcanic flows in the upper parts of the Jønland Formation are conformably overlain to the SE (towards Sunnsetkjølen and the Horg Fault; Fig. 2) by at least 300 m of greenish, predominantly thick-bedded, quartz-rich sandstones and granule conglomerates with mafic and felsic volcanic, jasper and quartzite clasts. We interpret the Sunnsetkjølen Formation to be a stratigraphic equivalent to the Nyplassen Formation (Fig. 3).

Fig. 5. Field photographs, upper parts of the Gåsbakken Formation, and the Nyplassen Formation. Locations are given in coordinate system WGS84, zone 32N. (**a**) Limestone with palaeokarst fractures or voids filled with rounded granule- and pebble-sized detritus. Note 2 cm rounded pebble in centre of photograph (E543883/N6994861). (**b**) Bedded limestone (upper left) and stratigraphically overlying (upside down) massive limestone (lower right). Foliation dips to the right (E551858/N7001477). (**c**) Fossiliferous limestone (E557283/N7001137). (**d**) Flaser- or lenticular-bedded shale and siltstone, upside down. Sandy beds <10 cm thick with planar lamination and subordinate cross-bedding or cross-lamination. Note trace fossils (P; *Planolites* isp.) and shell fragment (S; probably brachiopod) (M. Smelror, pers. comm. 2021) (E547194/N6998612). (**e**) Typical porphyrite with predominantly plagioclase phenocrysts. Phenocrysts are partly aligned parallel to bedding (E547295/N6998560). (**f**) Porphyrite with small phenocrysts of plagioclase (light) and pyroxene (dark). Original vesicles were filled with calcite that is weathered out (E547298/N6998649). (**g**) Porphyrite–limestone breccia stratigraphically below massive porphyrite (E552521/N6998764). (**h**) Contact between porphyrite and overlying siltstone or sandstone. Note the dark, slightly undulating, thin margin, originally the glassy surface, and the alignment of small plagioclase phenocrysts. The porphyrite is moderately amygdaloidal (E546238/N6994198). (**i**) Sandstone–siltstone (upside down) stratigraphically above porphyrite. Note planar lamination, cross-lamination and hummocky cross-bedding of the sandstones, indicating deposition above wave base in a shelf environment (E553222/N7000611). (**j**) Detail from Nyplassen Formation. Note basal erosive surfaces, normal grading and planar lamination in the sand and shale intervals (E545871/N6994045). (**k**) Detail from Nyplassen Formation (upside down). Note basal erosive surfaces, planar lamination and normal grading with pebble- or granule-size clasts at bottom and coarse sand at top (E545817/N6994049). (**l**) Nyplassen Formation, detail of granule conglomerate. Clasts of fine-grained felsic (white) and mafic (green) volcanic rocks, quartzite (light grey) and jasper (red) (E545817/N6994049).

Field relationships of the Raudhatten unit (Ilfjellet Group)

Conglomerates and sedimentary breccias of the Raudhatten unit in the Fjellvollen Formation of the Ilfjellet Group (Fig. 1b) contain clasts of porphyrites identical to those described above, pointing at a genetic link with the porphyrites in the Gåsbakken Formation of the Hølonda Group (Gasser *et al.* 2021). New field data and igneous geochemistry additionally indicate that the Raudhatten unit reflects a separate volcanic phase, subsequent to porphyrite

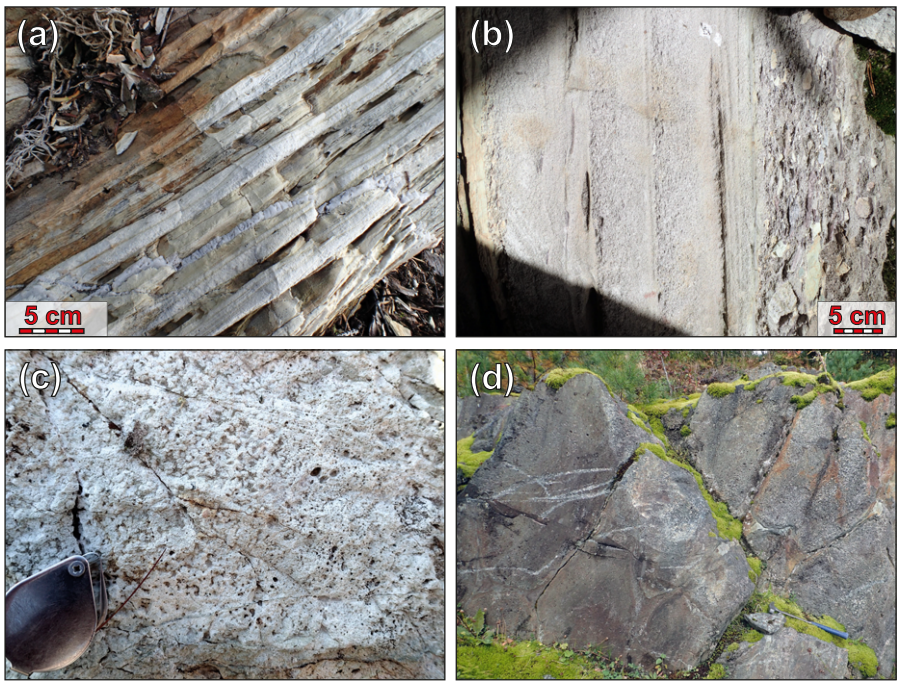

Fig. 6. Field photographs, Jønland and Sunnsetkjølen formations. Locations are given in coordinate system WGS84, zone 32N. (**a**) Thin-bedded sandstone–siltstone. Note planar lamination, cross-bedding and hummocky cross-bedding, indicating deposition above wave base in a shelf environment (E552681/N6995084). (**b**) Graded, reddish to greenish-grey sandstone–shale (left) and redbed pebbly breccia (right). Way up to the right (E547939/N6993877). (**c**) Dammen felsic flow. Amygdaloidal (right; weathered-out holes after calcite-filled vesicles). Spherulitic structures (left) (E552865/N6995850). (**d**) Amygdaloidal Dammen pillow lava (E554000/N6997162).

formation, but not known from currently studied parts of the Hølonda Group.

The Raudhatten unit comprises a generally upward-fining succession of conglomerates, breccias and tuffaceous deposits (Fig. 7a–f), forming a lens *c.* 200 m thick and at least 5 km long (Fig. 1b; Gasser *et al.* 2021). It locally shows an erosional base above underlying fine-grained (silt and sandy silt) turbidites and levee deposits, and rip-up clasts of calcareous sandstone (Fig. 7b) are common in conglomerates in lower parts of the unit. The conglomerate matrix is sandy to silty, containing compositionally homogeneous mafic tuffaceous material with little terrigenous input. Clasts include abundant porphyrite (Fig. 7a), limestone and varying proportions of jasper, igneous rocks and quartzite. Moderately amygdaloidal mafic volcanic

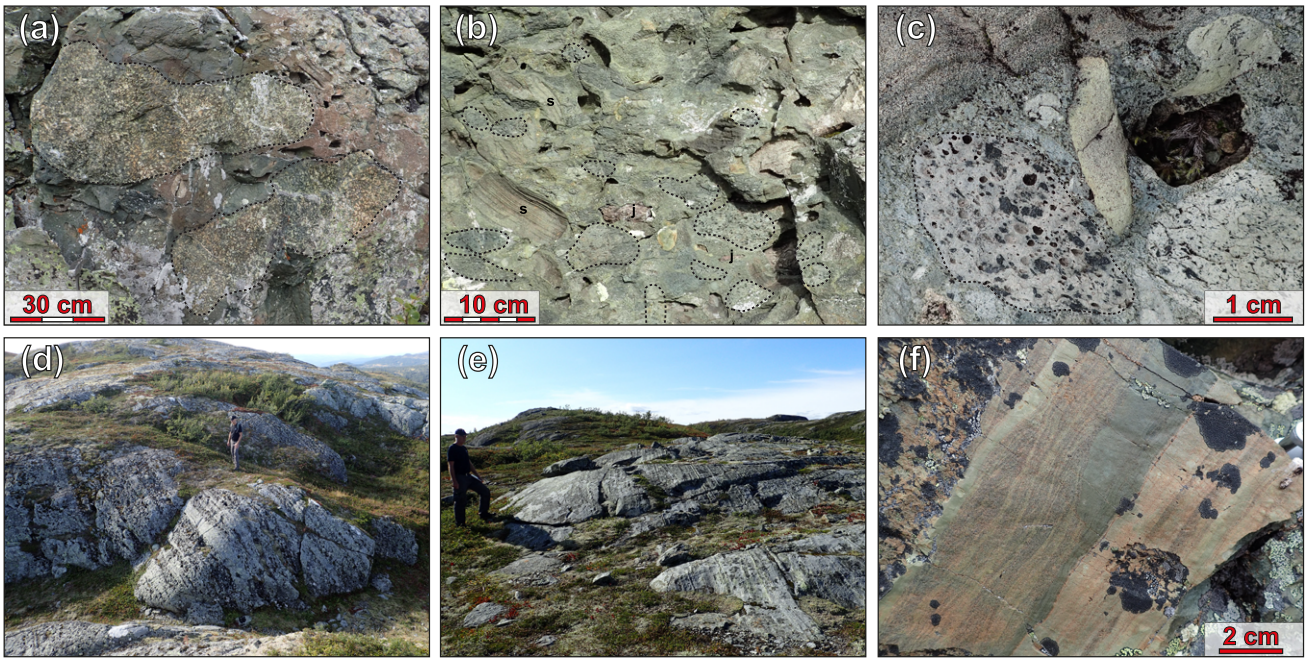

Fig. 7. Field photographs of the Raudhatten unit of the Ilfjellet Group. Locations are given in coordinate system WGS84, zone 32N. (**a**) Large blocks of porphyrite (outlined) in homogeneous tuff matrix. Weathered-out limestone clasts in upper right (E547297/N6985188). (**b**) Raudhatten conglomerate. Clasts of hornblende-phyric (dark specks) mafic volcanic rock (outlined) in homogeneous tuff matrix. Rip-up clasts of calcareous sandstone (*s*). Reddish jasper clasts (*j*). Cavities are from weathered-out limestone clasts (E547406/N6985220). (**c**) Close-up of hornblende-phyric volcanic rock (outlined) in Raudhatten conglomerate–breccia; abundant roundish holes are weathered-out, originally calcite-filled, amygdules. Larger hole on the right is from weathered-out limestone clast (E547224/N6985051). (**d**) Conglomerate–breccia beds (with abundant weathered-out limestone clasts) alternating with massive tuff beds (E543930/N6983160). (**e**) Bedded tuff overlying thick layer of massive tuff (left) (E543934/N6983172). (**f**) Close-up of cross-laminated fine-grained tuff in upper part of the Raudhatten unit (E547158/N6984939).

clasts characterized by euhedral hornblende phenocrysts (Fig. 7b and c) are abundant.

The lower part of the unit comprises homogeneous, thick-bedded to weakly stratified coarse-grained conglomerate and breccia beds with angular to slightly rounded pebbles, cobbles and boulders up to 1 m across. Both matrix- and clast-supported varieties are present. Conglomerate beds several metres thick alternate with coarse- to very coarse-grained tuffaceous sandstone beds up to 1 m thick that locally show weak cross-stratification and/or horizontal stratification. Channels up to 3 m deep are filled with coarse-grained massive to tabular bedded material. These deposits pass upwards into coarse to very coarse-grained tuffaceous sandstones alternating with conglomerate or breccia layers (Fig. 7d). The sandy intervals are mostly massive, locally containing outsized clasts, but horizontally stratified and cross-stratified varieties also occur. Upward fining from conglomerate to tuffaceous sandstone is common.

The middle to upper parts of the Raudhatten unit are dominated by bedded tuffaceous sandstone (Fig. 7e) and, ultimately, tuffaceous siltstone. Individual beds are generally thinner upwards, ranging from commonly >30 cm in middle parts (locally cut by up to 1 m deep channels) to decimetres and centimetres in upper parts (Fig. 7f). Sedimentary structures include normal grading, trough cross-bedding, planar and cross-lamination, scoured bases and load structures. Cross-bedding indicates sediment transport from a northwesterly source area.

Igneous geochemistry

The igneous rocks related to the Hølonda Group comprise at least six groups with distinctive whole-rock geochemical characteristics. We present data from five pillow lavas and associated sills of the Lo–Boggo unit, 12 volcanic rocks of the Nonsåsen unit, 18 porphyrites, and 13 volcanic rocks of the Dammen unit. For comparison, we also include two porphyritic dykes and five felsic dykes cutting the LVB ophiolite at Løkken, and one felsic dyke cutting the Mostadmarka Formation of the adjacent Ilfjellet Group.

Whole-rock data were obtained by XRF and laser ablation inductively coupled mass spectrometry (LA-ICP-MS) at the Geological Survey of Norway. Twenty-four samples were analysed for Nd and Sr isotopes by thermal ionization mass spectrometry (TIMS) at the British Geological Survey. All analytical data are found in Supplementary material 1; detailed analytical methods have been given by Gasser *et al.* (2021).

Felsic dykes

The felsic dykes cutting the LVB ophiolite at Løkken, including one dyke dated at 468.2 ± 0.7 Ma (Slagstad *et al.* 2014), and a similar dyke cutting the Mostadmarka Formation of the Ilfjellet Group, have uniform chemical compositions, clustering around 69% SiO_2 (Supplementary material 1) and within or close to the rhyolite field in the total alkalis–silica (TAS) diagram (Fig. 8a). Al_2O_3 is relatively high for felsic rocks (15.1–17.1%; Supplementary material 2). Notably, Y and heavy REE (HREE) are very low (e.g. 3.4–5.8 ppm Y; 0.29–0.49 ppm Yb). Chondrite- and mantle-normalized diagrams show steep patterns with high La/Lu_N ratios (*c.* 13 to 21), negligible or small positive Eu anomalies (Eu/Eu* 0.99–1.15), significant negative Nb–Ta anomalies and moderately negative Ti anomalies (Fig. 9). Contents of Sr are relatively high and show significant positive Sr anomalies in extended mantle-normalized plots for all but one sample (Supplementary material 3).

The felsic dykes have εNd_{468} values between 3.5 and 4.1, slightly more evolved than MORB in the Ilfjellet Group, which yielded values between 4.8 and 9.4 (Gasser *et al.* 2021), but with similar initial $^{87}Sr/^{86}Sr$ (Sr_i) between 0.7042 and 0.7059 (Fig. 10a). The Nd isotope composition is similar to that of the coeval Byneset trondhjemite dykes in the Bymarka ophiolite (Slagstad *et al.* 2014).

Whole-rock geochemical characteristics of the felsic dykes, including a lack of negative Eu anomalies (Fig. 9a), are in most respects similar to those of high-SiO_2 adakites (Supplementary material 2); in particular, the very low HREE and Y concentrations, combined with steep REE patterns and relatively high Sr, are diagnostic for adakite formation, requiring a garnet-rich and plagioclase-poor residue during partial melting (Castillo 2012; Zhang *et al.* 2021).

Lo–Boggo volcanic unit

The pillow lavas and sills of the Lo–Boggo unit are mostly mafic (Fig. 8a and b). Concentrations of MgO (up to 9.8%), Cr (up to 768 ppm) and Ni (up to 234 ppm) are high (Supplementary material 1). The rocks plot only slightly above the MORB–OIB (mid-ocean ridge basalt–ocean island basalt) array in the Th/Yb v. Nb/Yb diagram (Fig. 8c) of Pearce *et al.* (2014), close to basalts transitional between typical normal MORB (N-MORB) and E-MORB (E-MORB) compositions (Gale *et al.* 2013).

REE have nearly flat, upward-convex chondrite-normalized patterns (Fig. 9a), partly with a small enrichment of LREE (La/Lu_N 1.0–2.3). Compared with typical modern MORB, Lo–Boggo rocks have slightly elevated ratios of middle REE (MREE) to heavy REE (HREE) (Sm/Lu_N 1.2–2.4; Supplementary material 1), suggesting some influence of garnet in the melting source (Niu *et al.* 2001; Saccani *et al.* 2008; Wood *et al.* 2013). Mantle-normalized trace element patterns (Fig. 9b) are nearly flat and show no significant negative Nb–Ta anomaly.

The Lo–Boggo volcanic rocks have εNd_{467} of 5.7 and 7.0, similar to the MORB in the Ilfjellet Group, but with slightly higher Sr_i of 0.7066–0.7076 (Fig. 10a).

Nonsåsen volcanic unit

The Nonsåsen volcanic rocks are mostly of intermediate to felsic compositions, plotting in the trachyandesite and trachyte–trachydacite fields of the TAS diagram (Fig. 8a); two samples have rhyolitic compositions. The entire series is further classified as sodic in terms of K_2O/Na_2O proportions (Supplementary material 4). The trachyandesites thus are benmoreites based on standard classification schemes (Le Maître *et al.* 2002). The samples plotting in the trachyte–trachydacite field of the TAS diagram have normative quartz contents of *c.* 12–17% and are more akin to trachyte than to trachydacite.

The Th/Yb v. Nb/Yb diagram (Fig. 8c) demonstrates some similarity to continental arc rocks, although many samples extend beyond this field. Their enriched character in terms of highly incompatible trace elements is evident also in chondrite-normalized REE plots (Fig. 9a), with La/Lu_N ratios of *c.* 11–26 (Supplementary material 1). Mantle-normalized trace element compositions (Fig. 9b) also show steep patterns with strong enrichments of highly incompatible elements, significant negative Nb–Ta and positive Pb anomalies.

Notably, felsic Nonsåsen rocks have lower concentrations of REE than intermediate members (Fig. 9a). Significant Eu anomalies are virtually absent in all varieties. The marked decrease of highly incompatible elements such as Th, W, Nb and La with increasing SiO_2 (Fig. 11) is particularly striking; a similar decrease is seen for Pb (Fig. 9b and Supplementary material 1). Relationships between immobile elements, for example, strongly decreasing TiO_2 and highly incompatible trace elements at increasing SiO_2 (Fig. 11) whereas Al_2O_3 is nearly constant (Supplementary material 1), demonstrate that the most felsic varieties represent true rhyolitic compositions and are not the result of silicification or other alteration processes.

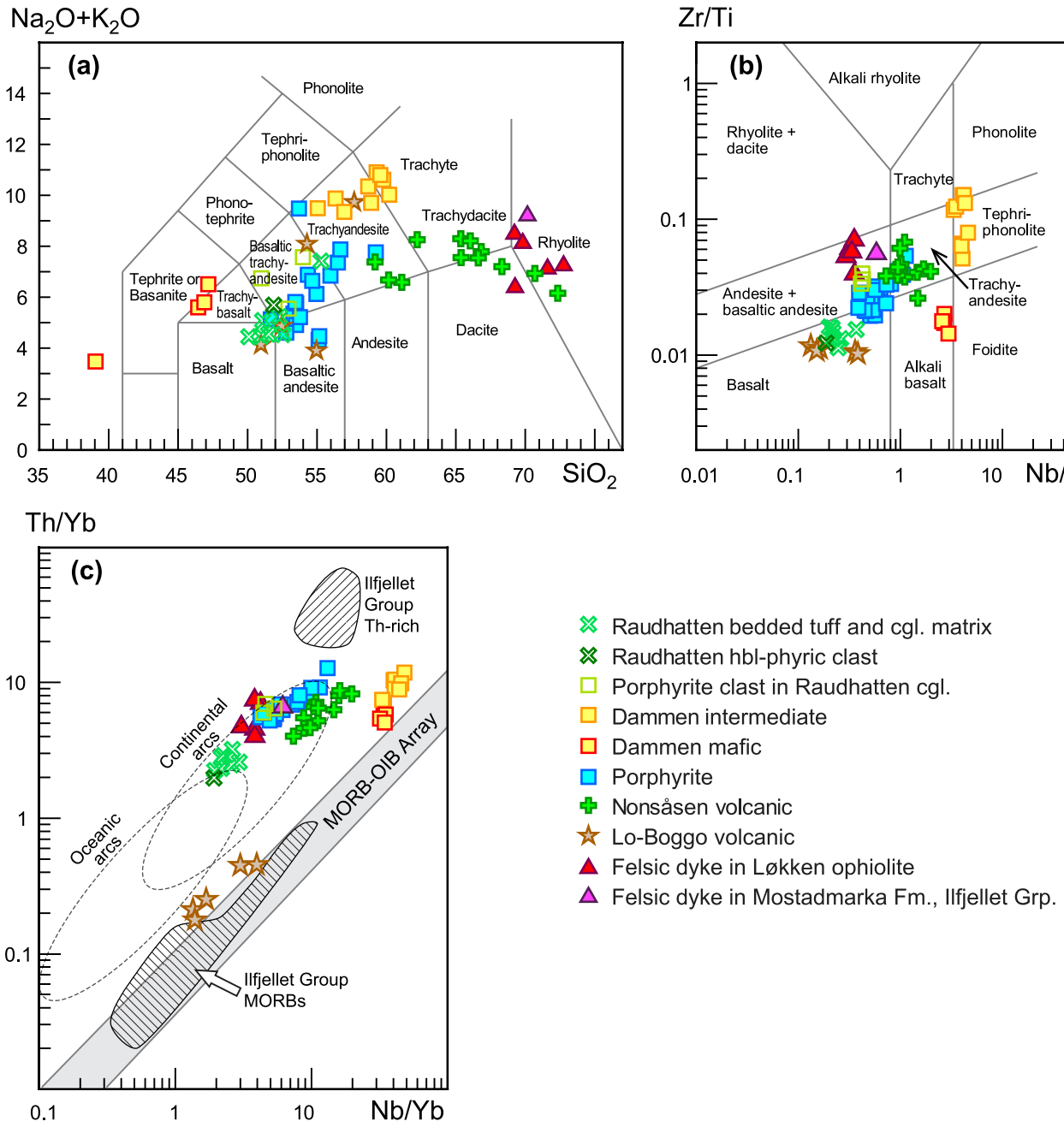

Fig. 8. Geochemical classification diagrams. (**a**) Total alkali–silica (TAS) diagram (Le Bas *et al.* 1986); (**b**) rock types (Pearce 1996); (**c**) Nb/Yb v. Th/Yb (Pearce 2008).

The Nonsåsen volcanic unit represents a compositionally distinctive series of effusive rocks with trace element ratios that exclude a common origin with the preceding adakitic and MORB-type magmas (Fig. 8c). Furthermore, the marked decrease of highly incompatible elements with increasing SiO_2 cannot be accounted for by fractional crystallization, because bulk partition coefficients would have been well below unity even if minor phases accommodated some of these elements at high SiO_2. Instead, negative linear trends may reflect magma mixing between an intermediate endmember with relatively high concentrations of incompatible trace elements and a felsic endmember with much lower concentrations. This would also be consistent with the lack of negative Eu anomalies, as well as generally larger positive Sr anomalies (Supplementary material 3) in the felsic members.

A hypothetical felsic endmember of the Nonsåsen magma series would have some geochemical similarities to the slightly older adakitic dykes (Fig. 11), including very low contents of highly incompatible trace elements and insignificant or slightly positive Eu anomalies, although markedly different in terms of Nb (>7.7 ppm in Nonsåsen rocks v. <2.1 ppm in the adakitic dykes; Fig. 11c and Supplementary material 1). The distinctly different trace element ratios are seen also in the larger negative Nb–Ta anomalies of the adakitic dykes and their different position in the Th/Yb v. Nb/Yb diagram (Fig. 8c).

The Nonsåsen volcanic unit has more evolved Nd isotopic compositions than the felsic dykes and the Lo–Boggo volcanic unit, with εNd_{467} between −0.7 and 2.0, whereas Sr_i is similar at 0.7049–0.7051 (Fig. 10a).

Porphyrites

The porphyrites are predominantly basaltic trachyandesites by TAS classification (Fig. 8a); trachyandesitic rocks are subordinate. They are further classified as potassic in terms of K_2O/Na_2O proportions

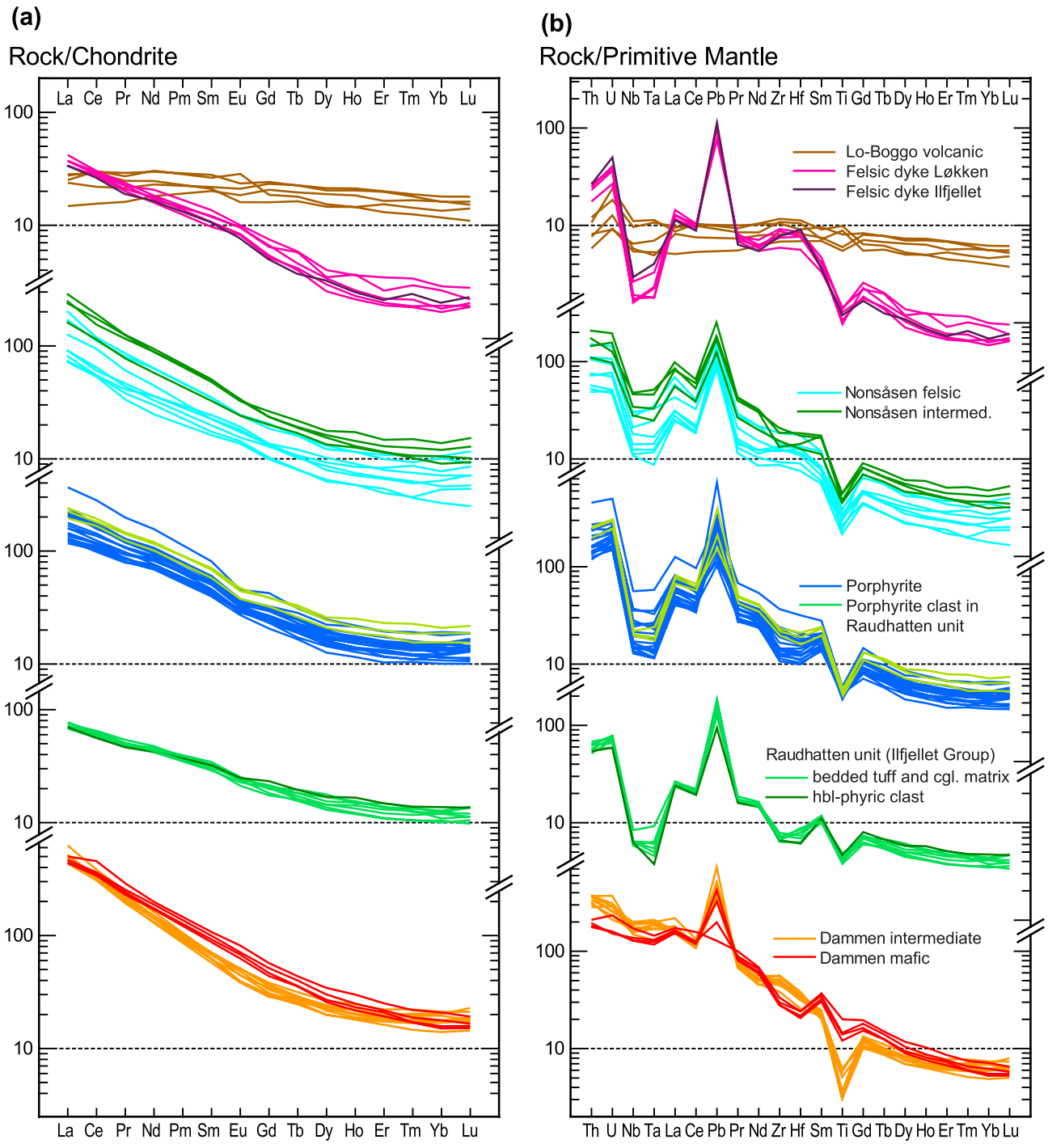

Fig. 9. Normalized trace element patterns. (**a**) Chondrite-normalized REE; (**b**) mantle-normalized trace elements. Normalizing values from Sun and McDonough (1989). Positive U anomalies in the Lo–Boggo unit reflect uptake during sub-seafloor alteration (MacDougall *et al.* 1979; Kelley *et al.* 2003), which significantly affects normalized trace element patterns for rocks with very low primary concentrations of U.

(Supplementary material 4) and hence are termed shoshonites and latites, respectively, based on traditional classification schemes (Le Bas *et al.* 1986). Th/Yb v. Nb/Yb ratios (Fig. 8c) plot in the extreme upper part of the field for typical continental arc rocks. Overall REE and mantle-normalized patterns are broadly similar to those of the Nonsåsen unit, including a strong enrichment of highly incompatible trace elements (e.g. La/Lu_N ratios of *c.* 10–20, Th enrichments (10–39 ppm), positive Pb anomalies, small negative or insignificant Eu anomalies, and significant negative Nb–Ta anomalies (Fig. 9 and Supplementary material 1). Still, distinctly different incompatible element ratios between the porphyrites and the Nonsåsen volcanic unit demonstrate unique magmatic signatures (e.g. Th/Yb v. Nb/Yb; Fig. 8c) that exclude derivation from a common parental magma through fractional crystallization, in accordance also with their different phenocryst mineralogy.

Incompatible elements generally show strong enrichments with increasing SiO_2 (Fig. 11), typically a three- to four-fold increase from mafic varieties to the most evolved latite at about 60% SiO_2. By contrast, TiO_2 shows only little enrichment over the same SiO_2 interval (Fig. 11), indicating significant fractionation of Fe–Ti oxides. The consistently negative Ti anomaly in mantle-normalized plots (Fig. 9b) also suggests that even the most mafic members of the porphyrites, at about 52% SiO_2, were not primary mantle-derived melts but must have undergone substantial fractionation.

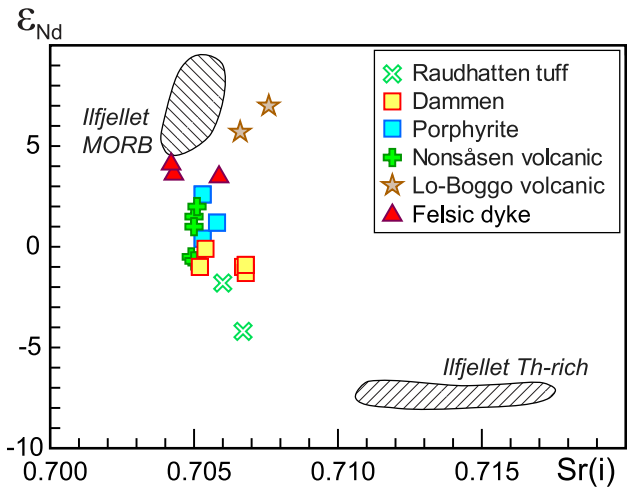

Fig. 10. Rb–Sr and Sm–Nd isotope data for the Hølonda volcanic rocks. Sample locations are shown in Figure 2. Initial Sr (Sr(i)) v. εNd, calculated for the time of crystallization determined by U–Pb zircon geochronology. Data from the Ilfjellet volcanic rocks are shown for comparison. Symbols as in Figure 8.

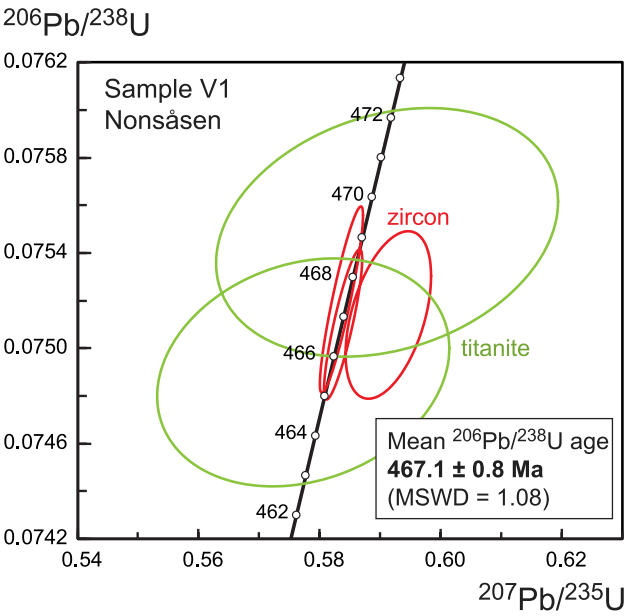

Fig. 12. Concordia plot for the zircon and titanite U–Pb thermal ionization mass spectrometry data of the Nonsåsen volcanic unit. Sample locations are shown in Figure 2. Data-point error ellipses are 2σ; plots are made with Isoplot (Ludwig 2003). MSWD, mean square weighted deviation.

The porphyrites have Nd and Sr isotopic compositions similar to the Nonsåsen volcanic unit, with εNd_{466} values between 0.4 and 2.6 and Sr_i of 0.7053–0.7058 (Fig. 10a). The range in Nd composition is similar to that previously reported by Slagstad *et al.* (2014).

Dammen volcanic unit

The Dammen volcanic unit is essentially bimodal, with a gap between mafic and intermediate members. By TAS classification (Fig. 8a), mafic lavas plot mostly on the boundary between trachybasalt and tephrite–basanite, whereas intermediate members plot in the upper parts of the trachyandesite and trachyte fields (Fig. 8a). An alkaline or ultra-alkaline character is supported by their position in the Zr/Ti v. Nb/Yb discriminant diagram of Pearce (1996), close to the foidite field for mafic members and within the tephriphonolite and phonolite fields for intermediate members (Fig. 8b). Concentrations of strongly incompatible trace elements are high (e.g. Th 15–32 ppm, Nb 91–142 ppm, La 105–150 ppm; in mafic members TiO_2 and P_2O_5 contents are up to 4.31 and 1.25%, respectively (Supplementary material 1).

The mafic lavas have low and highly variable K/La and Rb/Th ratios, reflecting large losses of mobile potassium and rubidium during alteration (Supplementary material 3). Such depletion patterns are typical of altered leucite-bearing igneous rocks, where leucite has rapidly degraded to analcime (Prelević *et al.* 2004). This process is potentially significant for rock classification of the Dammen rocks, as it creates a substantial shift towards lower total alkalis/SiO_2 ratios in the TAS diagram (Giampaolo *et al.* 1997). On this basis, it is likely that most mafic Dammen rocks were originally well inside the tephrite–basanite compositional field. Normative

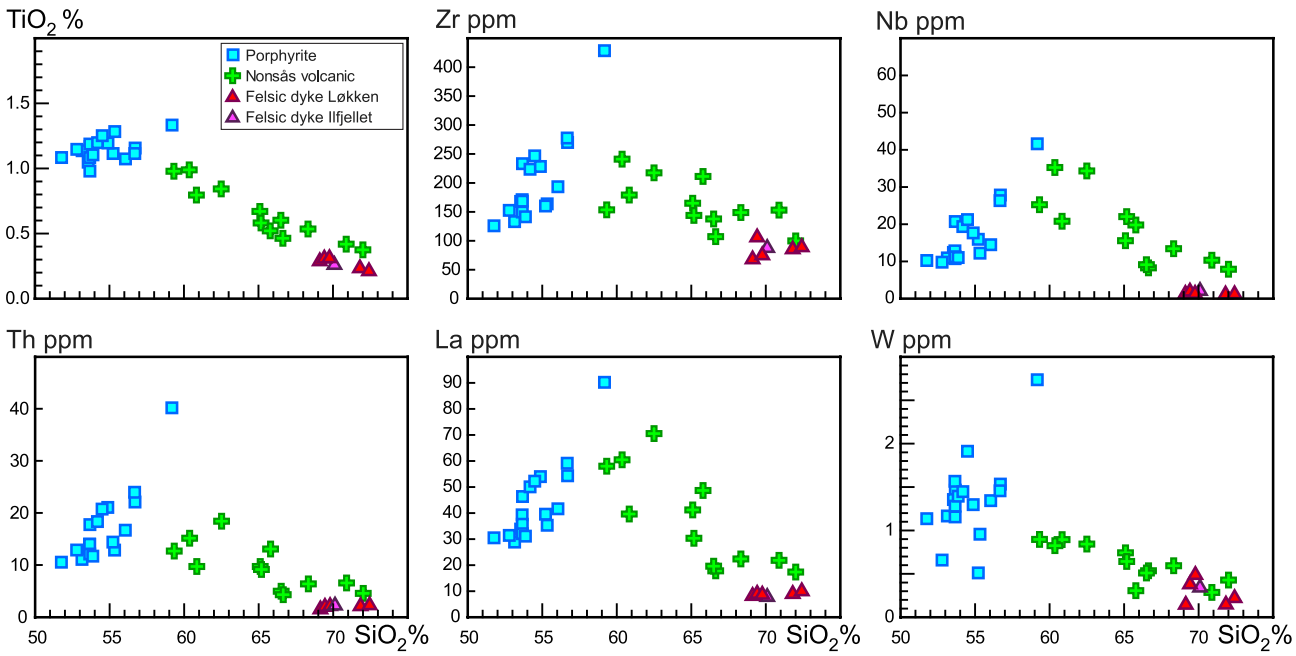

Fig. 11. Whole-rock geochemical variations of the Nonsåsen volcanic unit trends, with porphyrites and felsic dykes shown for comparison.

olivine contents are mostly well above 10% (up to 22%) and point to basanitic rather than tephritic compositions in terms of traditional classification schemes (Le Bas *et al.* 1986).

In the Th/Yb v. Nb/Yb diagram (Fig. 8c), the mafic Dammen rocks plot slightly above the upper part of the MORB–OIB array (Pearce 2014). REE patterns (Fig. 9a) display strong enrichment of LREE, with La/Lu_N ratios of 28–29 and no Eu anomaly. Mantle-normalized trace element patterns (Fig. 9b) show similar strong enrichments in highly incompatible trace elements, with insignificant or very small negative Nb–Ta anomalies. Negative Ti anomalies, together with low Cr (≤46) and Ni (≤45) contents indicate that the mafic Dammen members were not primary mantle-derived magmas but were significantly modified by fractional crystallization.

Intermediate members also have geochemical signatures demonstrating loss of K_2O (Supplementary material 3), indicating that they may have experienced a similar shift towards lower alkalis/

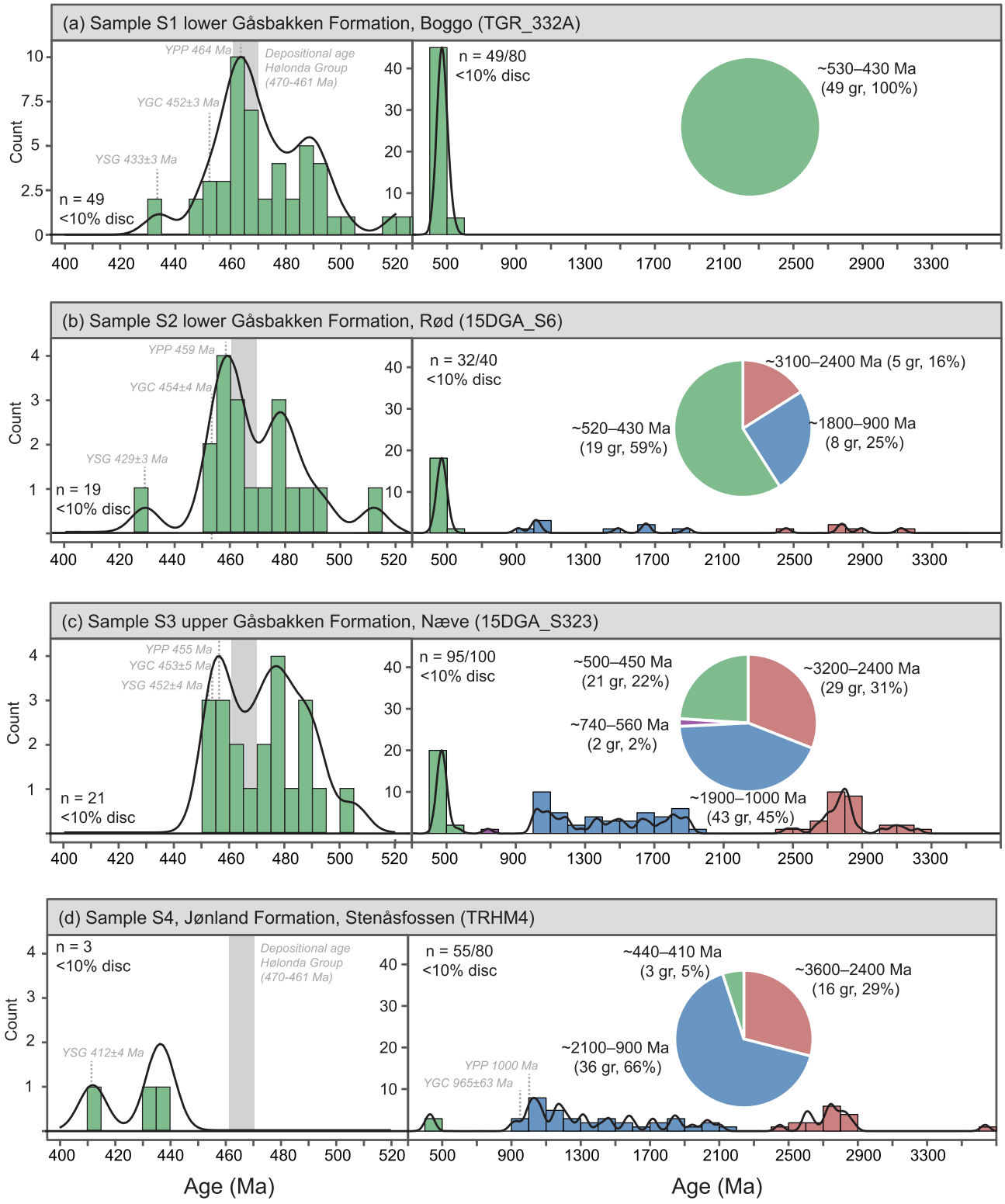

Fig. 13. Histograms, kernel density estimates and pie charts for four detrital zircon samples from the Hølonda Group. Sample locations are shown in Figure 2. For the left-hand plots, bin- and bandwidths are five; for the right-hand plots, binwidth is 100 and bandwidth is 25. n, number of included analyses; gr, grains. Plots are made with the detzrcr software of Andersen *et al.* (2018).

SiO_2 ratios in the TAS diagram (Giampaolo *et al.* 1997; Prelević *et al.* 2004) from originally tephriphonolite and phonolite. This would be in accordance with the classification diagram of Pearce (1996) based on the stable elements Zr, Ti, Nb and Yb (Fig. 8b). Although unequivocal discrimination between phonolite and trachyte based on the latter diagram is problematic owing to a large overlap (Pearce 1996; GEOROC database; https://georoc.mpch-mainz.gwdg.de//georoc/), the high Al_2O_3 contents of the Dammen intermediate rocks (up to 21.1%; Supplementary material 1) are clearly in favour of phonolitic and tephriphonolitic origins.

Normalized trace element patterns (Fig. 9) are nearly parallel for mafic and intermediate members of the Dammen unit, suggesting a common origin by fractional crystallization. Compared with the mafic members, the intermediate members show a moderate relative enrichment of Th–U, Nb–Ta and Zr–Hf whereas MREE are slightly depleted. Along with a significant relative depletion of Ti in the intermediate lavas, these trends are similar to the geochemical evolution of basanite to phonolite in modern examples (e.g. Ablay *et al.* 1998; Johansen *et al.* 2005), consistent with significant fractionation of hornblende and titanite.

The Dammen volcanic unit is slightly more evolved than the Nonsåsen volcanic unit and porphyrites in terms of Nd isotopes, but with overlapping εNd values between −1.3 and −0.1 (Fig. 10a). Sr_i is similar for all three, ranging from 0.7052 to 0.7068 (Fig. 10a) in the Dammen unit.

Raudhatten unit (Ilfjellet Group)

We present data from three porphyrite clasts from the Raudhatten unit for comparison with the porphyrites of the Hølonda Group. We also present data from seven samples of the conglomerate or breccia matrix and the bedded tuffaceous sedimentary rocks, as well as from one hornblende-phyric clast of the Raudhatten unit.

The typically plagioclase-phyric porphyrite clasts of the Raudhatten unit overlap with the porphyrites of the Hølonda Group (Figs 8 and 9). The only difference is that the Raudhatten samples are marginally more evolved in terms of Zr/Ti ratios (Fig. 8b) and one sample has slightly higher contents of HREE.

The hornblende-phyric mafic clast is compositionally nearly identical to the bedded tuffaceous sedimentary rocks and the conglomerate or breccia matrix, and significantly different from that of the plagioclase-phyric porphyrite clasts. They are predominantly mafic (Fig. 8a) and plot in the upper (relatively evolved) part of the basaltic field in the Nb/Yb v. Zr/Ti discrimination diagram (Fig. 8b), clearly different from porphyrite compositions. REE patterns (Fig. 9a) show moderate LREE enrichments (La/Lu_N ratios of *c.* 5–7, compared with 9–20 in the porphyrites) and insignificant Eu anomalies. Mantle-normalized plots (Fig. 9b) display negative Nb–Ta and positive Pb anomalies, but the most incompatible elements are less enriched than in the porphyrites (e.g. Th *c.* 4–6 ppm, compared with 10–39 ppm). The difference from the latter is seen also in the Th/Yb v. Nb/Yb diagram (Fig. 8c), where the tuffaceous sedimentary rocks and the conglomerate matrix are comparable with calc-alkaline rather than shoshonitic rocks (Pearce 1983).

A marginal deviation in Th/Yb–Nb/Yb ratios and REE patterns from the hornblende-phyric clast to the samples of tuffaceous sedimentary rocks and the conglomerate matrix (Figs 8c and 9a) may be explained by a small (mostly <10%) component of porphyrite detritus. The homogeneous compositions of the tuffaceous sedimentary rocks and the conglomerate matrix, and their similarity to the hornblende-phyric volcanic clast, indicate that they are dominated by juvenile volcanic material representing a distinctive magmatic phase. A near absence of terrigenous detrital material is in accordance with a lack of recoverable zircons.

The Raudhatten unit has the most evolved Nd isotopic compositions in this study, with εNd_{466} of −1.8 and −4.2, whereas Sr_i values of 0.7060 and 0.7067 are similar to those of the other units (Fig. 10a).

Geochronology

A sample of the Nonsåsen volcanic unit was dated by U–Pb isotope dilution thermal ionization mass spectrometry (ID-TIMS) on zircon and titanite. The analyses were performed at the Department of Geosciences at the University of Oslo, Norway. Zircon was chemically abraded, dissolved in HF at 195°C, and measured without prior chemical separation. Titanite was dissolved in HF in Savillex vials on a hot-plate and processed through a single-stage HCl–HBr chemical separation before measurements. Details of the procedure and parameters used have been described by Corfu (2004) and are given in Supplementary Table S5.

Three sandstone samples from the Gåsbakken Formation in the central Hølonda area and one sandstone sample from the stratigraphically equivalent Jønland Formation farther south were selected for detrital zircon LA-ICP-MS dating, aiming at characterizing the source areas and comparing maximum depositional age estimates with known fossil ages. The analyses were performed at the Geological Survey of Norway. A detailed description of the analytical methods has been given by Gasser *et al.* (2021), and the analytical data are given in Supplementary Table S6. Several attempts at separating zircons from the porphyrites, the Dammen volcanic unit and the Raudhatten matrix were unsuccessful.

U–Pb ID-TIMS dating of the Nonsåsen volcanic unit

Sample V1 (15DGA_S328) represents a pyroclastic unit with centimetre-sized fragments in a fine-grained matrix. The sparse zircon population consisted of small euhedral, short prismatic to equant crystals. Chemical abrasion rendered them cloudy, reflecting relatively high U contents. Titanite occurs as brown translucent fragments. Two single-grain zircon analyses overlap on concordia, whereas a third single-grain analysis is slightly discordant (Fig. 12). Two single titanite fragments yield data points that overlap on concordia but with larger errors than the zircon fractions. All five fractions give a mean $^{206}Pb/^{238}U$ age of 467.1 ± 0.8 Ma (MSWD = 1.08; Fig. 12).

LA-ICP-MS dating of detrital zircon

Sample S1 (TGR_332A) is a coarse-grained grey sandstone alternating with the Boggo black shale in the lower part of the Gåsbakken Formation (Fig. 2). Of the 80 grains analysed, 49 are <10% discordant and belong to a single Cambro-Ordovician age group (Fig. 13a). Different methods to estimate the maximum depositional age (MDA) give 433 ± 3 Ma (youngest single grain, YSG), 452 ± 3 Ma (youngest grain cluster, YGC, with $n \geq 3$ and 2σ overlap) and *c.* 464 Ma (youngest graphical probability peak, YPP; Fig. 13a). Details on methods for estimating MDA have been given by Coutts *et al.* (2019).

Sample S2 (15DGA_S6) is a fine-grained reddish Rød sandstone from the lower part of the Gåsbakken Formation (Fig. 2). The sample contained relatively few zircons. Of the 40 grains analysed, 32 are <10% discordant and fall into three general age groups: (1) Archean; (2) Paleo- to Mesoproterozoic; (3) Cambro-Ordovician (Fig. 13b). Different MDA methods give 429 ± 3 Ma (YSG), 454 ± 4 Ma (YGC) and *c.* 459 Ma (YPP; Fig. 13b).

Sample S3 (15DGA_S323) is a fine-grained grey sandstone grading into a dark grey siltstone at Næve, belonging to the Langåsvatnet member of the Gåsbakken Formation (Fig. 2). Of the 100 grains analysed, 95 are <10% discordant and fall into four general age groups: (1) Archean; (2) Paleo- to Mesoproterozoic; (3) Neoproterozoic (two grains at 739 ± 7 Ma and 566 ± 5 Ma); (4)

Cambro-Ordovician (Fig. 13c). Different MDA methods give 452 ± 4 Ma (YSG), 453 ± 5 Ma (YGC) and *c.* 455 Ma (YPP; Fig. 13c).

Sample S4 (TRHM4) is a greenish sandstone belonging to the Jønland Formation (Fig. 2). Of the 80 grains analysed, 55 are <10% discordant and fall into three general age groups: (1) Archean (including one very old grain of 3635 ± 34 Ma); (2) Paleo- to Mesoproterozoic; (3) Silurian (Fig. 13d). Different MDA methods give 412 ± 4 Ma (YSG), 965 ± 63 Ma (YGC) and *c.* 1000 Ma (YPP; Fig. 13c).

Summary and interpretation of the geochronological data

The U–Pb TIMS age of 467.1 ± 0.8 Ma for the Nonsåsen volcanic unit is the first radiometric age for volcanism in the Hølonda Group. It overlaps with the ages of 468.2 ± 0.7 and 467.4 ± 4.9 Ma for felsic dykes cutting the LVB ophiolite (Slagstad *et al.* 2014) and with the graptolite ages of the Lo and Boggo localities (*c.* 470–467 Ma; Schmidt-Gündel (1994)). The Nonsåsen age also corresponds well to the early to mid-Darriwilian (*c.* 466–465 Ma) conodont age of the stratigraphically overlying limestones (Bergström 1979) and the mid-Darriwilian (*c.* 465–461 Ma) graptolite age of the younger Nyplassen Formation. Together, the radiometric and faunal data constrain the depositional age of the Hølonda Group to *c.* 470–461 Ma (Fig. 13).

MDA estimates based on detrital zircon are mostly younger than the radiometric and faunal ages discussed above, except for the YPP estimate of sample S1 and the YGC and YPP estimates of sample S4 (Fig. 13). MDA estimates younger than the true depositional age have been observed in several datasets from Ordovician strata in the Trondheim Nappe Complex, probably resulting from hidden lead loss in the youngest grains owing to Silurian (Scandian) metamorphism (Dalslåen *et al.* 2021*a*, *b*; Gasser *et al.* 2021).

The detrital zircon populations indicate complex source areas, with the Cambro-Ordovician population probably derived from the underlying ophiolitic and associated arc successions (minor probability peaks at 480–490 Ma correspond to the age of the LVB ophiolite; Fig. 13), whereas the Mesoproterozoic to Archean populations probably represent a complex continental source. The latter populations are difficult to assign to a particular continental area within the Baltica–Laurentia realm (e.g. Slagstad and Kirkland 2017), but the oldest Eoarchean grain of 3635 ± 34 Ma is most probably sourced from the Greenland (Laurentian) craton, as the Fennoscandian (Baltic) craton does not contain rocks of Eoarchean age (Hölttä *et al.* 2008), supporting the generally Laurentian affinity of the Hølonda Group rocks.

Discussion

In the following section, we first discuss the depositional environment and the tectonomagmatic evolution of the Hølonda Group in detail (Fig. 14) before outlining the larger-scale palaeogeographical implications (Fig. 15).

Depositional environment of the Hølonda Group

The Gåsbakken Formation; subaerial to shallow-marine sedimentation and volcanism in a tectonically active setting

The sedimentary rocks of the Gåsbakken Formation demonstrate a diverse depositional environment with strong lateral facies variations in a tectonically active setting dominated by rifting, also reflected by the adjoining Ilfjellet basin (Gasser *et al.* 2021). The redbed deposits (Rød member) of the Gåsbakken Formation, including conglomerate and breccia as well as lenticular-bedded sandstone and shale, are interpreted to represent alternating channel and levee deposits in a fluvial to deltaic and shallow-marine environment (Fig. 14a). Some breccia or conglomerate beds may represent either debris flows, or continental sheet flows or sheet floods.

Clast composition, including ophiolitic detritus, felsic volcanic rocks and quartzite, indicates derivation from a source area comprising subaerially weathered, obducted ophiolite and associated arc rocks, as well as older continental elements, in accordance with the detrital zircon data. Abundant clasts of limestone are of unknown provenance; however, the association of redbeds with local limestone beds points to a possible source in coeval reef or shelf limestones (Fig. 14a). Numerous clasts of felsic volcanic rocks in the redbed deposits are also of unknown origin, but the feldspar-phyric texture may indicate a relationship to either the adakitic dykes or the Nonsåsen volcanic rocks.

Stratigraphic transitions from redbed type breccias, conglomerates and sandstones to limestone and local black shales, and vice versa, reflect periods of alternating subsidence and uplift and rapid shifts, both temporally and laterally, in the local depositional environment. This probably occurred in an extensional setting with faulting and associated footwall uplift processes (e.g. Gawthorpe and Leeder 2000). Black, graptolitic shales were deposited in fault-bounded basins with restricted water circulation (Fig. 14a).

The intermediate to felsic Nonsåsen volcanic unit is the most prominent volcanic unit within the lower part of the Gåsbakken Formation. Resting partly on grey and black shale (e.g. at Boggo), the initial Nonsåsen volcanism was submarine at least in places. Other parts of the Nonsåsen unit have features suggestive of subaerial volcanism, including autobrecciated lava (Fig. 4f and g) and air-fall pyroclastic deposits (Fig. 4i). Internal conglomerates dominated by well-rounded cobbles and boulders of Nonsåsen-like rocks (Fig. 4j) demonstrate considerable reworking of local volcanic material prior to final deposition, possibly by alluvial transport or in a beach environment (Fig. 14a). Angular to subangular limestone clasts reflect the existence of coeval and less reworked limestone.

Poorly sorted conglomerates on the western parts of the Nonsåsen volcanic unit (Fig. 4k), passing upwards into graded conglomerate and sandstone, were suggested by Ryan *et al.* (1980) to evince subaqueous deposition of subaerially weathered volcanic rocks. Together with overlying karstified limestone (Fig. 4l), the succession probably reflects reef or limestone deposition on a shallow shelf, followed by subaerial exposure and karst dissolution. Overlying shales indicate subsequent subsidence and deposition in a shallow-marine, tidally influenced environment.

The mode of emplacement of the porphyrites, a controversial question in earlier literature (Vogt 1945; Chadwick *et al.* 1963; Chaloupsky 1970; Bruton and Bockelie 1980; Grenne and Roberts 1998), is of particular interest. Our observations of their great lateral extent along one stratigraphic level, typically between underlying limestone and overlying thin-bedded, grey sandstone and shale, indicates that most porphyrites were emplaced as coherent volcanic flows. This is supported by a lack of peperite or other evidence of intrusive relationships at the hanging-wall contacts, which would be expected if they were emplaced as sills (Skilling *et al.* 2002).

The absence of pillows or other submarine lava structures is in favour of subaerial rather than submarine eruptions (Fig. 14b). Their generally coherent character and an apparent scarcity of flow breccias may be ascribed to their dominantly mafic compositions and low viscosity (e.g. McPhie *et al.* 1993). The great thickness of individual flow units is noteworthy in view of the inferred rift setting (Gasser *et al.* 2021), which potentially facilitated ponding of lava in local grabens. This scenario would be partly comparable with the deposition of thick, porphyritic lavas of latitic and shoshonitic composition in pull-apart basins at the edge of the Basin and Range Province (Busby *et al.* 2018). A rift setting is also consistent with the presence of swarms of extensive and very thick porphyrite dykes cutting the LVB ophiolite; the orientation of these

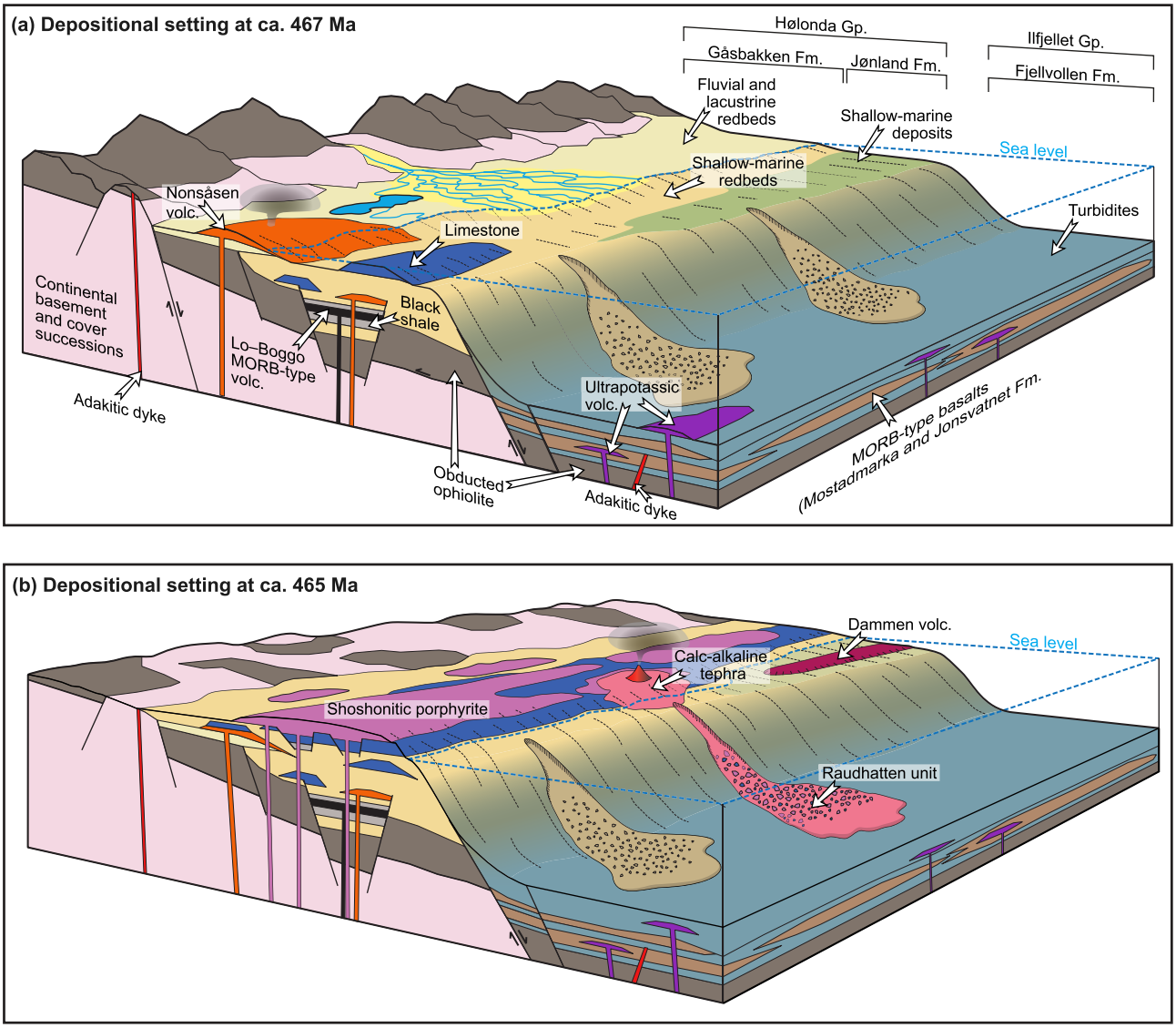

Fig. 14. (**a**) Depositional setting during formation of the Rød redbeds and the Nonsåsen volcanic rocks, lower part of the Gåsbakken Formation of the Hølonda Group (left) and the Fjellvollen Formation of the Ilfjellet Group (right). (**b**) Depositional setting during formation of the porphyrites and the Dammen volcanic rocks, upper part of the Gåsbakken Formation of the Hølonda Group (left) and the Fjellvollen Formation of the Ilfjellet Group (right). The volcanic source of the Raudhatten deposits (Fjellvollen Formation) is depicted at an inferred intermediate position.

dykes suggests an original SW–NE trend of fissure vents and by inference also of the rift-related basins.

Palaeokarst in underlying limestone demonstrates uplift and exposure, in accordance with subaerial conditions during the voluminous lava eruptions (Fig. 14b). In this context, the porphyrite–limestone breccias (Fig. 5g) at the contact with underlying limestone may be interpreted as reflecting the incorporation and partial assimilation of karstified and partially fragmented limestone into the hot lava. Limestone assimilation by mafic and intermediate magmas has been documented in shallow intrusive systems (e.g. Deegan *et al.* 2010; Carter and Dasgupta 2016) and by experimental assimilation in shoshonitic melts at low to intermediate pressures (Jolis *et al.* 2013). A similar process at a lava–limestone contact is consistent with a subaerial setting, as ambient seawater and a wet substrate would probably lead to rapid chilling below temperatures required for assimilation.

Thin-bedded sandstone and shale in the uppermost parts of the Gåsbakken Formation imply resumption of shallow-marine conditions after porphyrite eruptions, probably in a shelf environment. Sandstone–shale with hummocky cross-stratification and soft sediment deformation indicate deposition above storm wave base on a shallow (tidally influenced?) shelf dissected by channels. Sandstones and shales of the overlying Langåsvatnet member indicate further transgression and deposition in a deeper shelf or prodelta environment.

The Jønland Formation; an oceanward correlative of the Gåsbakken Formation

The stratigraphically lower parts of the Jønland Formation contain redbed breccias and sandstones identical to those of the Rød member in the Gåsbakken Formation. The distinctiveness of these rocks indicates that the two formations are stratigraphic equivalents. In contrast to the central Hølonda area, the redbed deposits in the Jønland Formation form generally thinner and finer-grained units interbedded with mostly greyish sandstones and shales, passing laterally northeastwards into thin-bedded, partly hummocky cross-bedded, grey sandstone and shale interpreted to represent a shallow shelf environment with occasional input of fine sand (Fig. 14a).

Lenticular-bedded shales in the upper parts of the Jønland Formation, near Dammen (Fig. 2a), may reflect a transition, at least

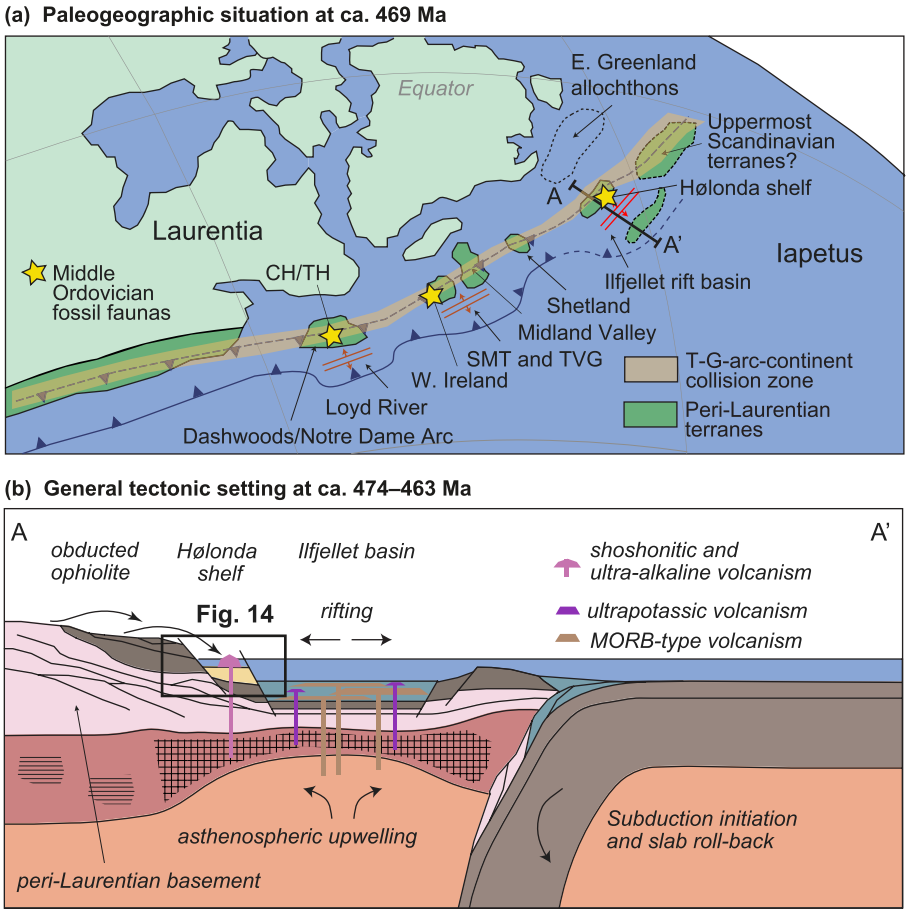

Fig. 15. (**a**) Palaeogeographical situation at *c.* 469 Ma; general outline modified from Domeier (2016). CH, Cow Head; G, Grampian; SMT, South Mayo Trough; T, Taconic; TH, Table Head; TVG, Tyrone Volcanic Group. (**b**) General tectonic setting of the Hølonda–Ilfjellet shelf and rift basin at *c.* 474–463 Ma (after Gasser *et al.* 2021).

locally, to a distal delta environment. A high vesicularity of the Dammen pillow basalts is in accordance with a shallow-marine setting. The precise age of the volcanic unit is unknown owing to a lack of datable zircons. However, stratigraphic relationships to the overlying Sunnsetkjølen Formation are comparable with those between the porphyrites and the Nyplassen Formation south of Nonsåsen (Figs 2 and 3), suggesting that the Dammen and the porphyrite magmatism were broadly contemporaneous (Fig. 14b) and older than the mid-Darriwilian (*c.* 466–461 Ma) graptolites of the Nyplassen Formation (Ryan *et al.* 1980).

We interpret the Jønland Formation as being deposited in an intermediate palaeogeographical position between those of the Gåsbakken Formation to the NW and the coeval Fjellvollen formation of the Ilfjellet Group farther SE, representing a transitional shelf setting (Fig. 14).

The Raudhatten unit; linking the Hølonda and Ilfjellet groups

The Raudhatten unit of the Ilfjellet Group, with its high content of short distance-transported porphyrite and limestone clasts, provides additional information on the depositional setting and volcanic evolution following porphyrite volcanism. Our new data indicate that the tuffaceous matrix of the Raudhatten conglomerates and associated tuffaceous bedded deposits are almost purely volcanic, representing fine-grained and minor blocky tephra of probably pyroclastic origin from a calc-alkaline volcanic phase distinctly different from the porphyrites (Fig. 14b). The predominance of fine-grained volcanic material in the Raudhatten conglomerate matrix indicates that it was derived from juvenile, unconsolidated tephra in the source area. Further, the abundance of porphyrite and limestone clasts in the lowermost Raudhatten conglomerates indicates that these rocks were exposed in the source area at the time of tephra deposition but had no time to degrade and contribute significantly to fine-grained sediment flux.

The characteristics of the Raudhatten unit, combined with the setting envisaged for the porphyrites, indicate deep-marine resedimentation of subaerial, syn-eruptive volcaniclastic deposits (McPhie *et al.* 1993). Equivalent primary volcanic deposits are not exposed in the studied areas, neither in the Hølonda Group nor in the Ilfjellet Group, hence their exact mode of deposition cannot be determined. However, strombolian- or vulcanian-type explosive eruptions are most likely, in view of the mafic composition and an apparent lack of highly vesicular, pumiceous or scoriaceous pyroclasts (McPhie *et al.* 1993). This scenario may have involved erosion of subaerial coastal and inland juvenile tephra, followed by debris avalanches (e.g. Carey and Schneider 2011) that also included porphyrite, limestone and exotic clasts (Fig. 14b).

The timing of Raudhatten deposition is not precisely constrained, but its characteristics indicate that it formed shortly after porphyrite emplacement, when deposits of the Hølonda Group were still subaerially exposed. As direct volcanic equivalents to the Raudhatten calc-alkaline tuffs have not been observed in the studied parts of the Hølonda Group, we speculate that this source area, with local, explosive volcanism, might have been in an intermediate or along-strike palaeogeographical position between that of the Ilfjellet Group and the currently exposed Hølonda Group.

Nyplassen, Sunnsetkjølen and Føssjøen formations; transition to turbiditic deposition

The Nyplassen Formation marks a notable transition from the subaerial to shallow-marine setting of the Gåsbakken Formation, to generally deeper-water, mass flow-controlled slope deposition. This transition was probably the result of tectonic subsidence combined with an increased clastic input from an emerging land mass with

varying source rocks exposed. The Nyplassen Formation is thought to represent deposition on a submarine fan, partly in the inter-channel and levee areas of the mid-fan, partly in upper fan channels.

The Sunnsetkjølen Formation is a stratigraphic equivalent to the Nyplassen Formation, indicating that deposits of the central Hølonda area and the southeastern transitional area had become part of the same turbiditic slope system. Similarly, the Føssjøen Formation of the Ilfjellet Group (Gasser *et al.* 2021) resembles the Nyplassen and Sunnsetkjølen formations with respect to both composition and sedimentary facies characteristics, suggesting that the upper parts of the Hølonda and Ilfjellet groups belonged to the same slope system after subsidence of the Gåsbakken shelf.

Tectonomagmatic evolution of the Hølonda Group

D- to E-MORB and adakitic magmatism; mantle upwelling and associated lower-crustal melting during post-collisional rifting

Felsic dykes of adakitic affinity, dated at 468.2 ± 0.7 Ma (Slagstad *et al.* 2014), cut the LVB ophiolite as well as the Mostadmarka Formation of the adjacent Ilfjellet Group, postdating ophiolite obduction and providing additional evidence for a link between the Hølonda and Ilfjellet successions. Comparable volcanic rocks are not observed in the Hølonda Group, but the abundance of texturally similar felsic clasts in the Rød breccias indicates that eruptive equivalents were eroded during or prior to deposition of the Rød redbeds.

Generation of adakitic magmas, requiring high-pressure partial melting to account for the presence of garnet and absence of plagioclase in the residue, was originally interpreted to reflect partial melting of garnet amphibolite or eclogite in descending young and hot oceanic slabs in subduction zones (Defant and Drummond 1990). Recent alternative models, however, include partial melting in lower continental crust (Castillo 2012; Dai *et al.* 2017; Zhang *et al.* 2021, and references therein).

The latter is most viable considering the recent tectonic model for the region (Gasser *et al.* 2021). Here, extensional opening of the related Ilfjellet basin led to asthenospheric mantle upwelling as reflected by D- to E-MORB-type magmatism from *c.* 474 Ma to at least 469 Ma in the adjacent Ilfjellet Group. Comparable volcanism of transitional D- to E-MORB signature with similar indications of minor crustal contamination is present in the Lo–Boggo volcanic unit (*c.* 470–467 Ma) in lower parts of the Hølonda Group.

The Lo–Boggo basalts, associated with graptolitic shales that partly may date back to 470 Ma, are broadly contemporaneous with the adakitic dykes. A link between the MORB-type magmatism and adakite generation is thus likely and may have included partial melting of lower crustal rocks owing to underplating by the mantle-derived MORB-type magma. This is in agreement with the model of Slagstad (2003), who argued that the corresponding 'Byneset trondhjemites' in the LVB ophiolite reflect partial melting at the base of a thick pile of amphibolitized mafic rocks stacked onto continental rocks during ophiolite obduction. It is also consistent with a slightly more evolved Nd isotopic composition for the adakitic dykes.

The Nonsåsen, porphyrite, Dammen and Raudhatten volcanic units; magmas from a variably metasomatized mantle

The Nonsåsen, porphyrite, Dammen and Raudhatten units represent distinct volcanic episodes that occurred within a relatively short, mid-Ordovician time span at *c.* 467–465 Ma. The shoshonitic porphyrites of the Hølonda Group have earlier been interpreted as being related to a continental island arc (Grenne and Roberts 1998). However, similar shoshonitic rocks exist in a variety of geotectonic settings, including oceanic and continental arcs, post-collisional belts and within-plate settings (Müller *et al.* 1992). In the adjacent Ilfjellet and equivalent Trollhøtta groups, shoshonitic to ultrapotassic volcanic rocks have been interpreted to represent partial melts of previously enriched mantle domains in a rift setting following arc–continent collision and ophiolite obduction (Dalslåen *et al.* 2020, 2021*b*; Gasser *et al.* 2021). Dalslåen *et al.* (2020) also proposed that the porphyrites of the Hølonda Group were related to the ultrapotassic rocks of the Ilfjellet and Trollhøtta groups, having formed on the shelf-side of an inferred rift basin.

Igneous rock suites similar to those of the Nonsåsen, porphyrite, Dammen and Raudhatten volcanic units are common in the circum-Tyrrhenian region of the Mediterranean (Peccerillo 2005; Conticelli *et al.* 2010; Mattei *et al.* 2010), where they are generally thought to involve small degrees of partial melting of enriched mantle. Also, the central Mediterranean equivalents are closely associated with ultrapotassic volcanic rocks comparable with those of the Ilfjellet and Trollhøtta groups (Dalslåen *et al.* 2020, 2021*a*; Gasser *et al.* 2021).

The Nonsåsen, porphyrite, Dammen and Raudhatten units are slightly younger than the ultrapotassic rocks of the Ilfjellet and Trollhøtta groups (*c.* 467–465 Ma v. *c.* 474–469 Ma). The Dammen unit is observed only within the Jønland Formation and represents a palaeogeographical position between those of the main Gåsbakken shelf and the Ilfjellet basin (Fig. 14b).

Isotopic data from the Nonsåsen, porphyrite, Dammen and Raudhatten units plot on a potential mixing line between an isotopically evolved (chemically enriched) source, represented by the 474–469 Ma ultrapotassic volcanic rocks in the Ilfjellet Group, and a juvenile source represented by the Ilfjellet and Lo–Boggo MORB (Fig. 10). Such a compositional and isotopic evolution, from ultrapotassic rocks with low $^{143}Nd/^{144}Nd$ and high $^{87}Sr/^{86}Sr$, to shoshonitic and calc-alkaline rocks with high $^{143}Nd/^{144}Nd$ and low $^{87}Sr/^{86}Sr$, has also been observed in the Tuscan and Roman magmatic provinces of the circum-Tyrrhenian area, where it is attributed to post-collisional isotherm relaxation (Conticelli *et al.* 2007, 2010).

We infer a petrogenetic origin for the Nonsåsen, porphyrite, Dammen and Raudhatten units similar to that of the central Mediterranean region, where the extreme compositional range of magmatic rocks reflects different melt batches with contributions from mantle domains variably enriched by fluids derived from subducting slabs and their sedimentary cover, influenced also by magma mixing and fractional crystallization (Lustrino *et al.* 2011, and references therein). In this scenario, the slightly older, ultrapotassic rocks of the related Ilfjellet and Trollhøtta groups may have resulted from partial melting of highly enriched, metasomatized veins in the lithospheric mantle at relatively low temperatures, whereas subsequent, less enriched magmas formed by partial melting of both veins and wall rocks at higher temperatures (Conticelli *et al.* 2007, 2010).

Palaeogeographical implications

The above detailed depositional and tectonomagmatic evolution can be placed within a larger palaeogeographical framework along the Ordovician margin of Laurentia (Fig. 15a; e.g. Bruton and Bockelie 1980; Neuman and Bruton 1989; Harper *et al.* 1996, 2009). The Laurentian margin was in late Neoproterozoic to early Cambrian times characterized by a wide hyperextended realm with detached continental blocks separated by transitional to oceanic crust (Chew and van Staal 2014; van Staal and Dewey 2022; van Staal and Zagorevski 2022). As a result of overall convergence between Laurentia and Gondwana, a south- to SE-dipping subduction zone developed outboard of the extended Laurentian margin from *c.* 515 Ma onwards, and a series of back-arc basins opened from *c.* 490 Ma as the result of slab rollback owing to the arrival of extended continental crust at the trench (van Staal and Dewey 2022).

The LVB ophiolite probably represents a comparable back-arc basin that was obducted as part of an arc–continent collision (Grenne and Roberts 1998; Slagstad *et al.* 2014; Gasser *et al.* 2021), possibly onto a peri-Laurentian continental fragment similar to the Dashwoods or Midland Valley terranes farther south (Fig. 15a). According to plate-tectonic reconstructions, an origin NE of corresponding peri-Laurentian faunas in Western Ireland and Newfoundland (Cow Head and Table Head), that is, near the Caledonian allochthons of present-day East Greenland, is most likely (Fig. 15a; Harper *et al.* 1996; Domeier 2016; Gasser *et al.* 2021). Because the latter represent passive margin sedimentation until *c.* 460 Ma (Smith and Rasmussen 2008), the early to mid-Ordovician LVB ophiolite and arc–continent collision must have occurred further outboard of, or possibly south of, the Greenland successions (Fig. 15a).

Ophiolite obduction and arc–continent collision occurred along the entire irregular Laurentian margin, followed by a diachronous subduction polarity reversal spanning from *c.* 475 Ma until 460 Ma, and the formation of several *c.* 475–465 Ma arc and back-arc complexes related to the new NW-verging slab (e.g. the Lloyds River, South Mayo Trough and Tyrone Volcanic Group basins, Fig. 15a; van Staal and Dewey 2022). The Ilfjellet basin adjacent to the Hølonda area, interpreted to represent an intermediate phase of rifting associated either with rollback and breakoff of the SE-dipping old slab (Dalslåen *et al.* 2020) or with rollback of the newly formed NW-dipping slab (Gasser *et al.* 2021), is apparently related to the same, orogen-scale, polarity flip.

In contrast to the early development of arc magmatism farther SW along the Caledonian–Appalachian orogen, polarity flip in the central Norwegian sector was not followed by proper arc magmatism (represented by the emplacement of calc-alkaline batholiths at *c.* 460 Ma; Meyer *et al.* 2003; Tucker *et al.* 2004) until significantly later. Moreover, the combined Hølonda–Ilfjellet basin was probably underlain by continental lithosphere (Fig. 15b), in contrast to contemporaneous, oceanic back-arc basins farther SW (Fig. 15a). The Hølonda–Ilfjellet basin, therefore, does not represent a classical Pacific-style back-arc setting. Instead, we envisage a setting similar to the central Mediterranean region. There, opening of the Tyrrhenian Sea was associated with mantle upwelling and MORB- to OIB-type magmatism (Peccerillo 2005), in a region of thickened orogenic lithosphere and a mantle enriched in incompatible elements during several previous subduction and collisional events (e.g. Di Stefano *et al.* 2009; Conticelli *et al.* 2013).

We speculate here that the Hølonda–Ilfjellet basin opened within a larger region of peri-Laurentian hyper-extended lithosphere outboard of Greenland, affecting the southernmost part of the terranes eventually thrust on top of the Caledonides of central and northern Norway. The latter nappes are generally thought to have originated from the northern end of the Taconian–Grampian arc–continent collisional system, showing evidence of a long-lived, Cambrian to Ordovician, continental-arc-related and collisional history (Fig. 15a; Yoshinobu *et al.* 2002; Roberts *et al.* 2007; Slagstad *et al.* 2021).

Conclusions

The stratigraphy of the newly defined Hølonda Group reflects a transition from subaerial and shallow-marine clastic and carbonate sedimentation on a continental shelf in the NW (Gåsbakken Formation) to deeper-water turbidite sedimentation along a subsiding continental slope towards the SE (Nyplassen Formation). The corresponding Jønland and Sunnsetkjølen formations represent a transitional shelf–slope setting.

Adakitic dykes intruded the LVB ophiolite and the adjacent Ilfjellet Group after ophiolite obduction and provide a link between the successions. Apart from these dykes, four distinct volcanic units were identified within the Hølonda Group: the Lo–Boggo MORB-type unit (*c.* 470–467 Ma), the benmoreitic to rhyolitic Nonsåsen unit (dated at 467.1 ± 0.8 Ma), and the shoshonitic porphyrites and the broadly coeval basanitic to trachytic or phonolitic Dammen unit (*c.* 465 Ma). The calc-alkaline Raudhatten unit of the adjacent Ilfjellet Group was temporally and palaeogeographically related to the shoshonitic porphyrites. Together with MORB and ultrapotassic volcanic units in the adjacent Ilfjellet and Trollhøtta groups (*c.* 474–470 Ma), the Hølonda volcanic rocks represent a mid-Ordovician volcanic suite comparable with equally complex igneous rock associations in the present-day central Mediterranean region.

A complex tectonic setting, also broadly comparable with the central Mediterranean region, is envisaged for the Hølonda, Ilfjellet and Trollhøtta groups near the northeastern Laurentian margin. Arc–continent collision and ophiolite obduction, probably onto a microcontinental block outboard of the main Laurentian continent (represented by the southern parts of the uppermost terranes of the central and northern Scandinavian Caledonides?), was followed by a subduction polarity flip and the establishment of a continent-dipping subduction zone. Rollback of the subducting slab led to rifting and the opening of a wide basin on thinned continental lithosphere from *c.* 474 Ma onwards, accommodating thick successions of turbidites, MORB and minor ultrapotassic volcanic rocks now found in the Ilfjellet and Trollhøtta groups (Dalslåen *et al.* 2020, 2021*a*; Gasser *et al.* 2021).

Further general subsidence and northwestward transgression, punctuated by periods of local footwall uplift in a tectonically active, extensional setting, initiated sedimentation on the adjacent Hølonda shelf after *c.* 470 Ma. This led to deposition of subaerial to shallow-marine sediments on the weathered and eroded ophiolite, reefs and calcareous deposits in shallow-marine areas, and anoxic black-shale sedimentation in restricted basins; concomitant volcanism varied from submarine to subaerial.

Deposition of the Hølonda Group ended with subsidence of the shelf and a transition to deeper-water turbiditic slope deposits. The Hølonda, Ilfjellet and Trollhøtta groups together represent a unique mid-Ordovician tectonomagmatic phase at the northeastern end of the Taconian–Grampian tract along the peri-Laurentian margin during the closure of the Iapetus Ocean.

Scientific editing by Christopher Barnes

Acknowledgements X-ray fluorescence analyses were performed by J. Schönenberger and A. E. Karlsen at the Geological Survey of Norway (NGU). Mineral separation was performed by A. Nordtømme, and thin sections were prepared by B. Johansen and B. Berge (all NGU). T. S. Røhr (NGU) assisted with LA-ICP-MS analysis of trace elements. I. Millar at the British Geological Survey, Keyworth, performed the Rb–Sr and Sm–Nd isotope analyses. We thank C. Busby, J. P. Nystuen, D. Roberts, P. D. Ryan and M. Smelror for discussions and input on earlier versions of the paper. J. Nelson and C. van Staal are thanked for constructive and thorough reviews.

Author contributions **TG**: conceptualization (lead), data curation (lead), formal analysis (lead), investigation (lead), writing – original draft (lead), writing – review & editing (lead); **DG**: conceptualization (equal), data curation (supporting), formal analysis (equal), investigation (equal), writing – original draft (equal), writing – review & editing (equal); **RB**: data curation (supporting), formal analysis (supporting), investigation (supporting), writing – review & editing (supporting); **FC**: data curation (equal), formal analysis (equal), writing – review & editing (supporting); **ØS**: data curation (equal), formal analysis (equal), writing – review & editing (supporting); **TS**: data curation (equal), formal analysis (equal), writing – review & editing (supporting)

Funding Fieldwork and analytical work were funded by Geological Survey of Norway.

Competing interests The authors declare that they have no known competing financial interests or personal relationships that could have appeared to influence the work reported in this paper.

Data availability All data generated or analysed during this study are included in this published article (and its supplementary information files).

References

Ablay, G.J., Carroll, M.R., Palmer, M.R., Marti, J. and Sparks, R.S.J. 1998. Basanite–phonolite lineages of the Teide–Pico Viejo volcanic complex, Tenerife, Canary Islands. *Journal of Petrology*, **39**, 905–936, https://doi.org/10.1093/petroj/39.5.905

Andersen, T., Kristoffersen, M. and Elburg, M.A. 2018. Visualizing, interpreting and comparing detrital zircon age and Hf isotope data in basin analysis – a graphical approach. *Basin Research*, **30**, 132–147, https://doi.org/10.1111/bre.12245

Bergström, S.M. 1979. Whiterockian (Ordovician) conodonts from the Hølonda Limestone of the Trondheim Region, Norwegian Caledonides. *Norsk Geologisk Tidsskrift*, **59**, 295–307.

Blake, D.H. 1962. A new lower Ordovician graptolite fauna from the Trondheim region. *Norsk Geologisk Tidsskrift*, **42**, 223–238.

Brøgger, W.C. 1875. Fossiler fra det Throndhjemske. *Nyt Magasin for Naturvidenskaberne*, **21**, 95–107.

Bruton, D.L. and Bockelie, J.F. 1980. Geology and paleontology of the Hølonda area, western Norway, a fragment of North America? *In*: Wones, D.R. (ed.) *The Caledonides in the USA*. **2**, Department of Geological Sciences, Virginia Polytechnic Institute and State University Memoirs, 41–47.

Bruton, D.L. and Bockelie, J.F. 1982. The Løkken–Hølonda–Støren areas. *In*: Bruton, D.L. and Williams, S.H. (eds) *Field Excursion Guide, 4th International Symposium on the Ordovician System*. Paleontological Contributions from the University of Oslo, 77–91.

Busby, C.J., Putirka, K., Melosh, B., Renne, P.R., Hagan, J.C., Gambs, M. and Wesoloski, C. 2018. A tale of two Walker Lane pull-apart basins in the ancestral Cascades arc, central Sierra Nevada, California. *Geosphere*, **14**, 2068–2117, https://doi.org/10.1130/GES01398.1

Carey, S.N. and Schneider, J.-L. 2011. Volcaniclastic processes and deposits in the deep-sea. *In*: Hüneke, H. and Mulder, T. (eds) *Deep Sea Sediments*. Elsevier, Amsterdam, **63**, 457–515, https://doi.org/10.1016/B978-0-444-53000-4.00007-X

Carter, L.B. and Dasgupta, R. 2016. Effect of melt composition on crustal carbonate assimilation: implications for the transition from calcite consumption to skarnification and associated CO_2 degassing. *Geochemistry, Geophysics, Geosystems*, **17**, 3893–3916, https://doi.org/10.1002/2016GC006444

Castillo, P.R. 2012. Adakite petrogenesis. *Lithos*, **134–135**, 304–316, https://doi.org/10.1016/j.lithos.2011.09.013

Chadwick, B., Blake, D.H., Beswick, A.E. and Rowling, J.W. 1963. The geology of the Fjeldheim–Gåsbakken area, Sør-Trøndelag. *Norges Geologiske Undersøkelse*, **223**, 43–60.

Chaloupsky, J. 1970. Geology of the Hølonda–Hulsjøen area, Trondheim Region. *Norges Geologiske Undersøkelse*, **266**, 277–304.

Chaloupsky, J. 1977. *Hølonda, bedrock map 1521 II 1:50 000*. Norges Geologiske Undersøkelse, Trondheim.

Chew, D.M. and van Staal, C.R. 2014. The ocean–continent transition zones along the Appalachian–Caledonian margin of Laurentia: examples of large-scale hyperextension during the opening of the Iapetus Ocean. *Geoscience Canada*, **41**, 165–185, https://doi.org/10.12789/geocanj.2014.41.040

Cohen, K.M., Finney, S.C., Gibbard, P.L. and Fan, J.-X. 2013. The ICS International Chronostratigraphic Chart. *Episodes*, **36**, 199–204, https://doi.org/10.18814/epiiugs/2013/v36i3/002

Conticelli, S., Carlson, R.W., Widom, E. and Serri, G. 2007. Chemical and isotopic composition (Os, Pb, Nd, and Sr) of Neogene to Quaternary calc-alkalic, shoshonitic, and ultrapotassic mafic rocks from the Italian peninsula: inferences on the nature of their mantle sources. *Geological Society of America, Special Papers*, **418**, 171–202, https://doi.org/10.1130/2007.2418(09)

Conticelli, S., Laurenzi, M.A. *et al.*. 2010. Leucite-bearing (kamafugitic/leucititic) and -free (lamproitic) ultrapotassic rocks and associated shoshonites from Italy: constraints on petrogenesis and geodynamics. *Journal of the Virtual Explorer*, **36**, https://doi.org/10.3809/jvirtex.2009.00251

Conticelli, S., Avanzinelli, R., Poli, G., Braschi, E. and Giordano, G. 2013. Shift from lamproite-like to leucititic rocks: Sr–Nd–Pb isotope data from the Monte Cimino volcanic complex vs. the Vico stratovolcano, Central Italy. *Chemical Geology*, **353**, 246–266, https://doi.org/10.1016/j.chemgeo.2012.10.018

Corfu, F. 2004. U–Pb age, setting and tectonic significance of the anorthosite–mangerite–charnockite–granite suite, Lofoten–Vesterålen, Norway. *Journal of Petrology*, **45**, 1799–1819, https://doi.org/10.1093/petrology/egh034

Coutts, D.S., Matthews, W.A. and Hubbard, S.M. 2019. Assessment of widely used methods to derive depositional ages from detrital zircon populations. *Geoscience Frontiers*, **10**, 1421–1435, https://doi.org/10.1016/j.gsf.2018.11.002

Dai, H.K., Zheng, J., Zhou, X. and Griffin, W.L. 2017. Generation of continental adakitic rocks: crystallization modeling with variable bulk partition coefficients. *Lithos*, **272–273**, 222–231, https://doi.org/10.1016/j.lithos.2016.12.020

Dalslåen, B.H., Gasser, D., Grenne, T., Augland, L.E. and Corfu, F. 2020. Ordovician shoshonitic to ultrapotassic volcanism in the central Norwegian Caledonides: the result of sediment subduction, mantle metasomatism and mantle partial melting. *Lithos*, **356–357**, 105372, https://doi.org/10.1016/j.lithos.2020.105372

Dalslåen, B.H., Gasser, D., Grenne, T., Augland, L.E. and Andresen, A. 2021*a*. Early–middle Ordovician sedimentation and bimodal volcanism at the margin of Iapetus: the Trollhøtta–Kinna basin of the Central Norwegian Caledonides. *Geological Society, London, Special Publications*, **503**, 251–277, https://doi.org/10.1144/SP503-2020-37

Dalslåen, B.H., Gasser, D., Grenne, T., Ganerød, M. and Andresen, A. 2021*b*. The Skuggliberga unit of the Oppdal area, central Scandinavian Caledonides: calc-alkaline pyroclastic volcanism in a fluvial to shallow-marine basin following a mid-Ordovician orogenic event. *Norwegian Journal of Geology*, **101**, https://doi.org/10.1785/njg101-2-2

Deegan, F.M., Troll, V.R., Freda, C., Misiti, V., Chadwick, J.P., McLeod, C.L. and Davidson, J.P. 2010. Magma–carbonate interaction processes and associated CO_2 release at Merapi volcano, Indonesia: insights from experimental petrology. *Journal of Petrology*, **51**, 1027–1051, https://doi.org/10.1093/petrology/egq010

Defant, M.J. and Drummond, M.S. 1990. Derivation of some modern arc magmas by melting of young subducted lithosphere. *Nature*, **347**, 662–665, https://doi.org/10.1038/347662a0

Di Stefano, R., Kissling, E., Chiarabba, C., Amato, A. and Giardini, D. 2009. Shallow subduction beneath Italy: three-dimensional images of the Adriatic–European–Tyrrhenian lithosphere system based on high-quality P wave arrival times. *Journal of Geophysical Research: Solid Earth*, **114**, 1–17, https://doi.org/10.1029/2008JB005641

Domeier, M. 2016. A plate tectonic scenario for the Iapetus and Rheic oceans. *Gondwana Research*, **36**, 275–295, https://doi.org/10.1016/j.gr.2015.08.003

Furnes, H., Roberts, D., Sturt, B.A., Thon, A. and Gale, G.H. 1980. Ophiolite fragments in the Scandinavian Caledonides. Proceedings International Ophiolite Symposium, 1979, Nicosia. Cyprus Geological Survey Department, 582–600.

Gale, A., Dalton, C.A., Langmuir, C.H., Su, Y. and Schilling, J.G. 2013. The mean composition of ocean ridge basalts. *Geochemistry, Geophysics, Geosystems*, **14**, 489–518, https://doi.org/10.1029/2012GC004334

Gasser, D., Grenne, T., Corfu, F., Bøe, R., Røhr, T.S. and Slagstad, T. 2021. Concurrent MORB-type and ultrapotassic volcanism in an extensional basin along the Laurentian Iapetus margin: tectonomagmatic response to Ordovician arc–continent collision and subduction polarity flip. *Geological Society of America Bulletin*, **134**, 1635–1659, https://doi.org/10.1130/b36113.1

Gawthorpe, R.L. and Leeder, M.R. 2000. Tectono-sedimentary evolution of active extensional basins B) C). 195–218.

Gee, D. 1975. A tectonic model for the central part of the Scandinavian Caledonides. *American Journal of Science*, **275**, 468–515, https://doi.org/10.2475/ajs.277.5.647

Gee, D.G., Roberts, D. and Wolff, F.C. 1985. The central–southern part of the Scandinavian Caledonides. *In*: Gee, D.G. and Sturt, B.A. (eds) *The Caledonide Orogen: Scandinavia and Related Areas*. Wiley, New York, 109–133.

Giampaolo, C., Godano, R.F., Di Sabatino, B. and Barrese, E. 1997. The alteration of leucite-bearing rocks: a possible mechanism. *European Journal of Mineralogy*, **9**, 1277–1292, https://doi.org/10.1127/ejm/9/6/1277

Grenne, T. 1980. Excursions across part of the Trondheim Region, Central Norwegian Caledonides: the Vassfjellet area. *Norges Geologiske Undersokelse*, **54**, 159–164.

Grenne, T. 1989. Magmatic evolution of the Løkken SSZ Ophiolite, Norwegian Caledonides: relationships between anomalous lavas and high-level intrusions. *Geological Journal*, **24**, 251–274, https://doi.org/10.1002/gj.3350240403

Grenne, T. and Roberts, D. 1998. The Hølonda Porphyrites, Norwegian Caledonides: geochemistry and tectonic setting of Early–Mid-Ordovician shoshonitic volcanism. *Journal of the Geological Society, London*, **155**, 131–142, https://doi.org/10.1144/gsjgs.155.1.0131

Gromet, L.P. and Roberts, D. 2010. Early Ordovician ages of zircons from felsic rocks and a conglomerate clast, Frosta peninsula, Central Norwegian Caledonides. *Norges Geologiske Undersøkelse Bulletin*, **450**, 60–64.

Gromet, L.P. and Roberts, D. 2016. U–Pb zircon ages of felsic rocks in the Forbordfjell ophiolite fragment, Støren nappe, Mid-Norwegian Caledonides. *Norsk Geologisk Tidsskrift*, **96**, 1–9, https://doi.org/10.17850/njg96-4-01

Harland, W.B. and Gayer, R.A. 1972. The Arctic Caledonides and earlier oceans. *Geological Magazine*, **109**, 289–314, https://doi.org/10.1017/S0016756800037717

Harper, D.A.T., Mac Niocaill, C. and Williams, S.H. 1996. The palaeogeography of early Ordovician Iapetus terranes: an integration of faunal and palaeomagnetic constraints. *Palaeogeography, Palaeoclimatology, Palaeoecology*, **121**, 297–312, https://doi.org/10.1016/0031-0182(95)00079-8

Harper, D.A.T., Owen, A.W. and Bruton, D.L. 2009. Ordovician life around the Celtic fringes: diversifications, extinctions and migrations of brachiopod and trilobite faunas at middle latitudes. *Geological Society, London, Special Publications*, **325**, 157–170, https://doi.org/10.1144/SP325.8

Heim, M., Grenne, T. and Prestvik, T. 1987. The Resfjell ophiolite fragment, southwest Trondheim region, central Norwegian Caledonides. *Norges Geologiske Undersøkelse Bulletin*, **409**, 49–72.

Hölttä, P., Balagansky, V. *et al.*. 2008. Archean of Greenland and Fennoscandia. *Episodes*, **31**, 13–19, https://doi.org/10.18814/epiiugs/2008/v31i1/003

Johansen, T.S., Hauff, F., Hoernle, K. and Kiel, D. 2005. Basanite to phonolite differentiation within 1550–1750 yr: U–Th–Ra isotopic evidence from the A.D. 1585 eruption on La Palma, Canary Islands. *Geology*, **33**, 897–900, https://doi.org/10.1130/G21663.1

Jolis, E.M., Freda, C., Troll, V.R., Deegan, F.M., Blythe, L.S., McLeod, C.L. and Davidson, J.P. 2013. Experimental simulation of magma–carbonate interaction beneath Mt. Vesuvius, Italy. *Contributions to Mineralogy and Petrology*, **166**, 1335–1353, https://doi.org/10.1007/s00410-013-0931-0

Kelley, K.A., Plank, T., Ludden, J. and Staudigel, H. 2003. Composition of altered oceanic crust at ODP Sites 801 and 1149. *Geochemistry, Geophysics, Geosystems*, **4**, https://doi.org/10.1029/2002GC000435

Kjær, J. 1932. The Hovin Group in the Trondheim area. Stratigraphical researches on the fossiliferous horizons in Meldalen, Hølandet and Gauldalen. *Det Norske Videnskapsakademi i Oslo Skrifter I. Matematisk-Naturvidenskapelig Klasse I*, **4**, 1–115.

Kjerulf, T. 1981. Om Trondheims stifts geologi (I). *Nyt Magasin for Naturvidenskaberne*, **18**, 1–78.

Le Bas, M.J., Le Maître, R.W., Streckeisen, A. and Zanettin, B. 1986. A chemical classification of volcanic rocks based on the total alkali–silica diagram. *Journal of Petrology*, **27**, 745–750, https://doi.org/10.1093/petrology/27.3.745

Le Maître, R., Streckeisen, A., Zanettin, B., Le Bas, M., Bonin, B., and Bateman, P. (eds) 2002. *Igneous Rocks: A Classification and Glossary of Terms: Recommendations of the International Union of Geological Sciences Subcommission on the Systematics of Igneous Rocks*, 2nd edn. Cambridge University Press, Cambridge, **236**, https://doi.org/10.1017/CBO9780511535581

Ludwig, K.R. 2003. A Geochronological Toolkit for Microsoft Excel. *Berkeley Geochronology Center Special Publications*, **4**, 70.

Lustrino, M., Duggen, S. and Rosenberg, C.L. 2011. The Central–Western Mediterranean: anomalous igneous activity in an anomalous collisional tectonic setting. *Earth-Science Reviews*, **104**, 1–40, https://doi.org/10.1016/j.earscirev.2010.08.002

MacDougall, J.D., Finkel, R.C., Carlson, J. and Krishnaswami, S. 1979. Isotopic evidence for uranium exchange during low-temperature alteration of oceanic basalt. *Earth and Planetary Science Letters*, **42**, 27–34, https://doi.org/10.1016/0012-821X(79)90187-0

Mattei, M., Conticelli, S. and Giordano, G. 2010. The Tyrrhenian margin geological setting: from the Apennine orogeny to the K-rich volcanism. *Special Publications of IAVCEI*, **3**, 7–27, https://doi.org/10.1144/IAVCEI003.2

McPhie, J., Doyle, M. and Allen, R. 1993. *Volcanic Textures A Guide to the Interpretation of Textures in Volcanic Rocks*. University of Tasmania, Centre for Ore Deposit and Exploration Studies, 196.

Meyer, G.B., Grenne, T. and Pedersen, R.B. 2003. Age and tectonic setting of the Nesåa Batholith: implications for Ordovician are development in the Caledonides of Central Norway. *Geological Magazine*, **140**, 573–594, https://doi.org/10.1017/S0016756803008069

Müller, D., Rock, N.M.S. and Groves, D.I. 1992. Geochemical discrimination between shoshonitic and potassic volcanic rocks in different tectonic settings: a pilot study. *Mineralogy and Petrology*, **46**, 259–289, https://doi.org/10.1007/BF01173568

Neuman, R.B. and Bruton, D.L. 1974. Early Middle Ordovician fossils from the Hølonda area, Trondheim Region, Norway. *Norsk Geologisk Tidsskrift*, **54**, 69–115.

Neuman, R.B. and Bruton, D.L. 1989. Brachiopods and trilobites from the Ordovician Lower Hovin Group (Arenig/Llanvirn), Hølonda area, Trondheim Region, Norway: new and revised taxa and paleogeographic interpretation. *Norges Geologiske Undersøkelse Bulletin*, **414**, 49–89.

Niu, Y., Bideau, D., Hékinian, R. and Batiza, R. 2001. Mantle compositional control on the extent of mantle melting, crust production, gravity anomaly, ridge morphology, and ridge segmentation: a case study at the Mid-Atlantic Ridge 33–35°N. *Earth and Planetary Science Letters*, **186**, 383–399, https://doi.org/10.1016/S0012-821X(01)00255-2

Nystuen, J.P. 1989. Rules and recommendations for naming geological units in Norway by the Norwegian Committee on Stratigraphy. *Norsk Geologisk Tidsskrift*, **69**, 1–111.

Pearce, J.A. 1983. Role of the sub-continental lithosphere in magma genesis at active continental margins. *In:* Hawkesworth, C.J. and Norry, M.J. (eds.) *Continental Basalts and Mantle Xenoliths, Nantwich, Cheshire*. Shiva Publications, 230–249.

Pearce, J. 1996. A user's guide to basalt discrimination diagrams. *In*: Wyman, D.A. (ed.) *Trace Element Geochemistry of Volcanic Rocks: Applications for Massive Sulphide Exploration*. Geological Association of Canada, Short Course Notes, **12**, 113.

Pearce, J.A. 2008. Geochemical fingerprinting of oceanic basalts with applications to ophiolite classification and the search for Archean oceanic crust. *Lithos*, **100**, 14–48, https://doi.org/10.1016/j.lithos.2007.06.016

Pearce, J.A. 2014. Immobile element fingerprinting of ophiolites. *Elements*, **10**, 101–108, https://doi.org/10.2113/gselements.10.2.101

Pearce, J.A., Hastie, A.R. *et al.*. 2014. Composition and evolution of the Ancestral South Sandwich Arc: implications for the flow of deep ocean water and mantle through the Drake Passage Gateway. *Global and Planetary Change*, **123**, 298–322, https://doi.org/10.1016/j.gloplacha.2014.08.017

Peccerillo, A. 2005. *Plio-Quaternary Volcanism in Italy: Petrology, Geochemistry, Geodynamics*. Springer, Berlin, **365**.

Pedersen, R.B., Bruton, D.L. and Furnes, H. 1992. Ordovician faunas, island arcs and ophiolites in the Scandinavian Caledonides. *Terra Nova*, **4**, 217–222, https://doi.org/10.1111/j.1365-3121.1992.tb00475.x

Prelević, D., Foley, S.F., Cvetković, V. and Romer, R. 2004. The analcime problem and its impact on the geochemistry of ultrapotassic rocks from Serbia. *Mineralogical Magazine*, **68**, 633–648, https://doi.org/10.1180/0026461046840209

Robert, B., Domeier, M. and Jakob, J. 2021. On the origins of the Iapetus ocean. *Earth-Science Reviews*, **221**, 103791, https://doi.org/10.1016/j.earscirev.2021.103791

Roberts, D. 1980. Petrochemistry and palaeogeographic setting of the Ordovician volcanic rocks of Smola, central Norway. *Norges Geologiske Undersokelse*, **359**, 43–60.

Roberts, D. 1982*a*. Disparate geochemical patterns from the Snasavatn greenstone, Nord-Trondelag, central Norway. *Norges Geologiske Undersokelse*, **373**, 63–73.

Roberts, D. 1982*b*. Rare earth element pattems from the Ordovician volcanites of Smøla, Nordmøre, west–central Norway. *Norsk Geologisk Tidsskrift*, **62**, 207–209.

Roberts, D. 1998. High-strain zones from meso- to macro-scale at different structural levels, Central Norwegian Caledonides. *Journal of Structural Geology*, **20**, 111–119, https://doi.org/10.1016/S0191-8141(97)00082-5

Roberts, D. and Tucker, R.D. 1998. Late Cambrian U–Pb zircon age of a metatrondhjemite from Ytteroya, Trondheimsfjorden, Central Norwegian Caledonides. *Norsk Geologisk Tidsskrift*, **78**, 253–258.

Roberts, D. and Wolff, F.C. 1981. Tectonostratigraphic development of the Trondheim region Caledonides, Central Norway. *Journal of Structural Geology*, **3**, 487–494, https://doi.org/10.1016/0191-8141(81)90048-1

Roberts, D., Walker, N., Slagstad, T., Solli, A. and Krill, A. 2002. U–Pb zircon ages from the Bymarka ophiolite, near Trondheim, Central Norwegian Caledonides, and regional implications. *Norsk Geologisk Tidsskrift*, **82**, 19–30.

Roberts, D., Nordgulen, Ø. and Melezhik, V. 2007. The uppermost allochthon in the Scandinavian Caledonides: from a Laurentian ancestry through Taconian orogeny to Scandian crustal growth on Baltica. *Geological Society of America, Memoirs*, **200**, 357–377, https://doi.org/10.1130/2007.1200(18)

Ryan, P.D., Williams, D.M. and Skevington, D. 1980. A revised interpretation of the Ordovician stratigraphy of Sør-Trøndelag, and its implications for the evolution of the Scandinavian Caledonides. *Department of Geological Sciences, Virginia Polytechnical Institute and State University, Memoir*, **2**, 99–106.

Saccani, E., Principi, G., Garfagnoli, F. and Menna, F. 2008. Corsica ophiolites: Geochemistry and petrogenesis of basaltic and metabasaltic rocks. *Ofioliti*, **33**, 187–207, https://doi.org/10.4454/ofioliti.v33i2.369

Schmidt, O. 1984. The graptolitic facies of the Bogo Shale (Arenig–Llanvirn), Sør-Trøndelag, west central Norway. *Geologica et Palaeontologica*, **18**, 17–19.

Schmidt, O. 1987. Lower Ordovician graptolite fauna of the Bogo Shale (West Norway), and its palaeogeographical relationships. *Bulletin of the Geological Society of Denmark*, **35**, 209–215, https://doi.org/10.37570/bgsd-1986-35-22

Schmidt-Gündel, O. 1994. *Die Unterordovizischen Graptolithenfaunen des Bogo- und des Lo-Schiefers (Sør-Trøndelag, West-Norwegen)*. Technical University Berlin.

Skilling, I.P., White, J.D.L. and McPhie, J. 2002. Peperite: a review of magma–sediment mingling. *Journal of Volcanology and Geothermal Research*, **114**, 1–17, https://doi.org/10.1016/S0377-0273(01)00278-5

Slagstad, T. 2003. Geochemistry of trondhjemites and mafic rocks in the Bymarka ophiolite fragment, Trondheim, Norway: petrogenesis and tectonic implications. *Norsk Geologisk Tidsskrift*, **83**, 167–185.

Slagstad, T. and Kirkland, C.L. 2017. The use of detrital zircon data in terrane analysis: a nonunique answer to provenance and tectonostratigraphic position in the Scandinavian Caledonides. *Lithosphere*, **9**, 1002–1011, https://doi.org/10.1130/L663.1

Slagstad, T., Pin, C. *et al.*. 2014. Tectonomagmatic evolution of the Early Ordovician suprasubduction-zone ophiolites of the Trondheim Region, Mid-Norwegian Caledonides. *Geological Society, London, Special Publications*, **390**, 541–561, https://doi.org/10.1144/SP390.11

Slagstad, T., Saalmann, K. *et al.*. 2021. Late Neoproterozoic–Silurian tectonic evolution of the Rödingsfjället nappe complex, orogen-scale correlations and implications for the Scandian suture. *Geological Society, London, Special Publications*, **503**, 279–304, https://doi.org/10.1144/SP503-2020-10

Smelror, M., Grenne, T., Gasser, D. and Bøe, R. 2022. Deep-water trace fossils in the Ilfjellet rift basin (Middle Ordovician), central Norwegian Caledonides. *Palaeoworld*, **32**, 63–78, https://doi.org/10.1016/j.palwor.2022.04.006

Smith, M.P. and Rasmussen, J.A. 2008. Cambrian–Silurian development of the Laurentian margin of the Iapetus Ocean in Greenland and related areas. *Geological Society of America, Memoirs*, **202**, 137–167, https://doi.org/10.1130/2008.1202(06)

Strand, T. 1949. New trilobites from the Hølonda limestone (Trondheim region, Southern Norway). *Norsk Geologisk Tidsskrift*, **27**, 74–88.

Sun, S.S. and McDonough, W.F. 1989. Chemical and isotopic systematics of oceanic basalts: implications for mantle composition and processes. *Geological Society, London, Special Publications*, **42**, 313–345, https://doi.org/10.1144/GSL.SP.1989.042.01.19

Tucker, R.D., Robinson, P. *et al.*. 2004. Thrusting and extension in the Scandian Hinterland, Norway: new U–Pb ages and tectonostratigraphic evidence. *American Journal of Science*, **304**, 477–532, https://doi.org/10.2475/ajs.304.6.477

van Staal, C.R. and Dewey, J. 2022. A review and tectonic interpretation of the Taconian–Grampian tract between Newfoundland and Scotland: diachronous accretion of an extensive forearc–arc–backarc system to a hyperextended Laurentian margin and subsequent subduction polarity reversal. *Geological Society, London, Special Publications*, **531**, https://doi.org/10.1144/SP531-2022-152

van Staal, C.R. and Zagorevski, A. 2022. Paleozoic tectonic evolution of the rifted margins of Laurentia. *Geological Society of America, Memoirs*, **220**, 1–18, https://doi.org/10.1130/2022.1220(24)

Vogt, T. 1945. The geology of part of the Hølonda–Horg district, a type area in the Trondheim Region. *Norsk Geologisk Tidsskrift*, **25**, 449–527.

Wilson, T.J. 1966. Did the Atlantic close and then re-open? *Nature*, **211**, 676–681, https://doi.org/10.1038/211676a0

Wood, B.J., Kiseeva, E.S. and Matzen, A.K. 2013. Garnet in the earth's mantle. *Elements*, **9**, 421–426, https://doi.org/10.2113/gselements.9.6.421

Yoshinobu, A.S., Barnes, C.G., Nordgulen, Ø., Prestvik, T., Fanning, M. and Pedersen, R.B. 2002. Ordovician magmatism, deformation, and exhumation in the Caledonides of central Norway: an orphan of the Taconic orogeny? *Geology*, **30**, 883–886, https://doi.org/10.1130/0091-7613(2002)030<0883:OMDAEI>2.0.CO;2

Zhang, L., Li, S. and Zhao, Q. 2021. A review of research on adakites. *International Geology Review*, **63**, 47–64, https://doi.org/10.1080/00206814.2019.1702592